UNCLASSIFIED

AD _ **405 111** __

DEFENSE DOCUMENTATION CENTER

FOR

SCIENTIFIC AND TECHNICAL INFORMATION

CAMERON STATION, ALEXANDRIA, VIRGINIA

UNCLASSIFIED

63_3_6

Reflection and Transmission of
Electromagnetic Waves from
Inhomogeneous Magnetoactive Plasma Slabs

29 MARCH 1963

Prepared by

RICHARD R. GOLD

Prepared for COMMANDER SPACE SYSTEMS DIVISION

UNITED STATES AIR FORCE

Inglewood, California

63 5

REFLECTION AND TRANSMISSION OF ELECTROMAGNETIC WAVES
FROM INHOMOGENEOUS MAGNETOACTIVE PLASMA SLABS

Prepared by

Richard R. Gold

AEROSPACE CORPORATION
El Segundo, California

Contract No. AF 04(695)-169

29 March 1963

Prepared for

COMMANDER SPACE SYSTEMS DIVISION
UNITED STATES AIR FORCE
Inglewood, California

63 5 185

ABSTRACT

Exact solutions for the reflection and transmission coefficients are obtained for two general electron density distributions: kinked-trapesoid (Fig. 1) and exponential-homogeneous-exponential (Fig. 5). Normal incidence into a stratified plasma slab is assumed so that the electromagnetic waves are propagating parallel to the free electron density gradients. A constant magnetic field is applied in the propagation direction. The solutions derived on this basis are used to evaluate the effect of the more realistic inhomogeneous plasma model, parametrically. Specific consideration is given to the analysis of transmission from a re-entry cone. The asymptotic expansion of the exact solution for the kinked-trapezoid profile provides a simplified expression for calculation purposes when L/λ_0 is larger than one. The analysis of problems in which L/λ_0 is much smaller than one is considered in some detail in the final section.

CONTENTS

FIGURES

SECTION I

INTRODUCTION

The general problem of the propagation of harmonic plane electro-magnetic waves in magnetoactive* plasmas was considered in Refs. 1 and 2. A brief review of the fundamental equations and a discussion of the problem of finding specific analytical solutions were presented. Detailed conclusions as to the effect of the applied magnetic field on transmission were based, primarily, on the parametric analysis of a homogeneous plasma slab. Preliminary consideration was also given to the more realistic inhomogeneous plasma model.

In a number of applications of current interest, the plasma contains free electron density gradients. For example, in microwave diagnostics of ionized gas flows in shock tubes, plasma tunnels, and fusion machines, the electromagnetic wave is caused to propagate from a dielectric into a dissipative medium through thermal boundary layers having such gradients. A similar situation is encountered by radar signals propagating to or from re-entry bodies. In this case, the radar signals may intercept ionized wakes also which are themselves inhomogeneous. The same problem exists in the now classical consideration of long radio waves entering the ionosphere.

In each case, if the electron density is slowly varying, a WKB approximation can be used to represent the propagation in the inhomogeneous region. If the transition distance between the dielectric and the homogeneous region is small compared to the plasma slab thickness, as is very often the case in the aforementioned laboratory work, then it is reasonable to assume complete homogeneity. In general, however, it will be necessary to examine the complete inhomogeneous plasma problem.

---

*This term is used to conveniently indicate the presence of an applied magnetic field.

The purpose of this report is to obtain the reflection and transmission coefficients for several exemplary transition zones between dielectric and dissipative gases. A number of formal solutions have been obtained[2] particularly in radio ionospheric research. However, relatively few boundary value problems have been treated in detail. We will restrict our attention to the case of normal incidence into a stratified medium such that the electromagnetic waves are propagating parallel to the free electron density gradients. The magnetic field is constant and is applied in the propagation direction.

The solutions derived on this basis are used to evaluate the effect of the more realistic inhomogeneous plasma model, parametrically, both with and without an applied magnetic field. At the same time, previously[2] obtained homogeneous plasma calculations for typical flight conditions can be refined accordingly. It should be noted that although the present problem is formulated in terms of ionized gas parameters, the equations and results are formally applicable to a variety of problems in other areas of interest — for example in the study of certain electromagnetic properties of solids.

SECTION II

FUNDAMENTAL EQUATIONS

The electromagnetic properties of a slightly ionised gas may be characterized by means of a conductivity function which linearly relates the current density and electric field strength. This function can be determined from the equation of motion for an average electron in some region of space in which is established, in general, a steady spatially dependent biasing magnetic field of induction $\vec{B}_0$:

$$m\frac{d\vec{v}}{dt} + m\omega_c \vec{v} = e(\vec{E} + \vec{v} \times \vec{B}_0) \quad , \tag{1}$$

where m is the electron mass, ω_c is the average electron collision frequency, $\vec{v}$ is the electron drift velocity, e the charge, and $\vec{E}$ is the electric field intensity. The force exerted by the magnetic field of the wave is neglected, harmonic time dependence of the form $\exp(i\omega t)$ for all time-varying vectors is assumed, and rationalized mks units are used.

A right-handed Cartesian coordinate system with the positive z-axis vertical is chosen, and the planes z = 0 and z = L constitute abrupt boundaries between free space in the regions z < 0 and z > L and the plasma in the region 0 < z < L. The plasma is assumed to be stratified so that its properties are functions only of z. We consider a plane wave from free space to be incident normally at the abrupt free space-plasma boundary z = 0, propagating into the medium with its wave-normal along the positive z-axis. Further, we assume that the applied magnetic field is in the direction of propagation and that the induction $\vec{B}_0$ is constant. Under the conditions noted above and using the relation

$$\vec{J} = Ne\vec{v} \quad , \tag{2}$$

where N is the number density of electrons, we can solve Eq. (1) for the current density $\vec{J}$. Substituting this expression into Maxwell's equations, we obtain the following governing equations for the propagation of the right- and left-handed circularly polarized waves[1]

$$F_r'' + n_0^2\left(1 - \frac{X}{U - Y}\right)F_r = 0 \quad , \quad F_\ell'' + n_0^2\left(1 - \frac{X}{U + Y}\right)F_\ell = 0 \quad , \quad (3)$$

$$G_r = -\frac{1}{n_0}F_r' \quad , \quad G_\ell = -\frac{1}{n_0}F_\ell' \quad , \quad (4)$$

where $n_0 = \omega/c_0 = 2\pi/\lambda_0$ is the free space wave propagation constant, λ_0 is the free space wavelength, and

$$F_r = E_x + iE_y \quad , \quad F_\ell = E_x - iE_y \quad , \quad E_z = 0 \quad , \quad (5)$$

$$G_r = \mathcal{H}_x + i\mathcal{H}_y \quad , \quad G_\ell = -\mathcal{H}_x + i\mathcal{H}_y \quad , \quad \mathcal{H}_z = 0 \quad . \quad (6)$$

Use is made of a modified magnetic field intensity $\vec{\mathcal{H}} = (\mu_0/\epsilon_0)^{1/2}\vec{H}$, where $(\mu_0/\epsilon_0)^{1/2} = c_0\mu_0$ is the free space impedance and c_0 is the velocity of light in vacuo. The angular plasma frequency ω_p and the angular cyclotron frequency at which the electrons gyrate due to the externally applied magnetic field $\vec{\omega}_B$ are given by

$$\omega_p^2 = \frac{Ne^2}{\epsilon_0 m} \quad , \quad \vec{\omega}_B = \frac{e\vec{B}_0}{m} \quad . \quad (7a)$$

The following nondimensional notation is introduced:

$$X = \left(\frac{\omega_p}{\omega}\right)^2 \quad , \quad \vec{Y} = \frac{\vec{\omega}_B}{\omega} \quad , \quad Z = \frac{\omega_c}{\omega} \quad , \quad U = 1 - iZ \quad , \quad (7b)$$

-4-

and the vector $\vec{Y}$ acts in the opposite direction to $\vec{B}_0$ (since $e < 0$) where $Y = |\vec{Y}| = |e| B_0 / m\omega$.

In the following sections, solutions are obtained to Eqs. (3) and (4) for several boundary value problems of interest in which the electron density distribution and, therefore X, is a known function of z. The collision frequency is assumed constant in all cases.[2] The general procedure for deriving these solutions and the specification of appropriate boundary conditions will be brought out in the separate analyses; note, however, that if we let

$$m_r = (U - Y)^{-1} \quad , \qquad m_\ell = (U + Y)^{-1} \quad , \tag{8}$$

then the equations for both the right- and the left-hand waves can be written in the form

$$F'' + n_0^2 [1 - mX(z)] F = 0 \quad , \tag{9}$$

$$G = -\frac{1}{n_0} F' \quad . \tag{10}$$

SECTION III

PROPAGATION IN INHOMOGENEOUS PLASMAS

A. Kinked-Trapezoid Electron Density Distribution

In order to evaluate the influence of an inhomogeneous plasma region on propagation, it is clearly desirable to be able to vary the character of the assumed profile while holding the remaining physical parameters fixed. Perhaps the simplest way of accomplishing this is shown in Fig. 1.[*] The transition regions $0 < z < z_1$, $z_2 < z < L$ connecting free space ($z < 0$, $z > L$) with a homogeneous plasma ($z_1 < z < z_2$) are represented by two straight-line segments. For simplicity the profile is assumed to be symmetric, i.e., $z_3 = L - z_0$ and $z_2 = L - z_1$. By varying the normalized transition dimension z_1/L, the location of the kink z_0/z_1, and the value of X at the kink X_0/X_1, while holding X_1, Z, Y, and L/λ_0 fixed, we can isolate the effect of the inhomogeneous plasma regions on reflection and transmission, parametrically.

Consider the following boundary value problem consistent with the description of Section II:

$$
\left.
\begin{aligned}
& F'' + n_0^2 \left[1 - mX(z) \right] F = 0 \quad ; \\
& m_r = (1 - Y - iZ)^{-1} \quad , \\
& m_\ell = (1 + Y - iZ)^{-1} \quad ,
\end{aligned}
\right\}
\tag{11}
$$

---

[*]This approach was suggested by Dr. R. Jahn in the course of several discussions of the general problem.

$$X(z) = 0 \quad , \quad z \leq 0 \quad ,$$

$$= X_0 z/z_0 \quad , \quad 0 \leq z \leq z_0 \quad ,$$

$$= X_0 + (X_1 - X_0)(z - z_0)/(z_1 - z_0) \quad , \quad z_0 \leq z \leq z_1 \quad ,$$

$$= X_1 \quad , \quad z_1 \leq z \leq z_2 \quad ,$$

$$= X_0 - (X_1 - X_0)(z - z_3)/(z_1 - z_0) \quad , \quad z_2 \leq z \leq z_3 \quad , \tag{12}$$

$$= -X_0(z - L)/z_0 \quad , \quad z_3 \leq z \leq L \quad ,$$

$$= 0 \quad , \quad z \geq L \quad .$$

The solutions in the several regions are as follows. For $z \leq 0$

$$F(z) = c^{(1)} e^{-in_0 z} + c^{(2)} e^{in_0 z} \quad . \tag{13}$$

For $0 \leq z \leq z_0$, Eq. (11) becomes

$$F'' + n_0^2 \left(1 - \frac{mX_0 z}{z_0} \right) F = 0 \quad .$$

Introducing the change of independent variables

$$\xi = -\left(\frac{n_0 z_0}{mX_0} \right)^{2/3} \left(1 - \frac{mX_0 z}{z_0} \right) \quad , \tag{14}$$

we obtain Stokes' equation

$$\frac{d^2 F}{d\xi^2} = \xi F$$

-7-

and, therefore, a solution in terms of Airy functions

$$F(\xi) = c^{(3)} \text{Ai}(\xi) + c^{(4)} \text{Bi}(\xi) \quad .$$ (15)

If we denote the index of refraction at the point $z = z_i$ by

$$K_i^2 = n^{*2}(z_i) = 1 - mX(z_i) = 1 - mX_i \quad ,$$ (16)

then in a similar manner, the substitution

$$\eta = -\left[\frac{n_0 K_0(z_1 - z_0)}{\left(1 - K_1^2/K_0^2\right)}\right]^{2/3}\left[1 - \left(1 - \frac{K_1^2}{K_0^2}\right)\left(\frac{z - z_0}{z_1 - z_0}\right)\right]$$ (17)

results in the solution, for $z_0 \leq z \leq z_1$,

$$F(\eta) = c^{(5)} \text{Ai}(\eta) + c^{(6)} \text{Bi}(\eta) \quad .$$ (18)

For the remaining regions: $z_1 \leq z \leq z_2$, $z_2 \leq z \leq z_3$, $z_3 \leq z \leq L$, $z \geq L$, respectively, the following solutions are obtained:

$$F(z) = c^{(7)} e^{-in_0 K_1 z} + c^{(8)} e^{in_0 K_1 z} \quad ,$$ (19)

$$F(\zeta) = c^{(9)} \text{Ai}(\zeta) + c^{(10)} \text{Bi}(\zeta) \quad ,$$ (20)

$$\zeta = -\left[\frac{n_0 K_0(z_1 - z_0)}{\left(1 - K_1^2/K_0^2\right)}\right]^{2/3}\left[1 + \left(1 - \frac{K_1^2}{K_0^2}\right)\left(\frac{z - z_3}{z_1 - z_0}\right)\right] \quad ,$$ (21)

$$F(v) = c^{(11)} \mathcal{A}i(v) + c^{(12)} \mathcal{B}i(v) \quad , \tag{22}$$

$$v = -\left(\frac{n_0 z_0}{mX_0}\right)^{2/3}\left[1 + \frac{mX_0(z - L)}{z_0}\right] \quad , \tag{23}$$

$$F(z) = c^{(13)} e^{-in_0 z} \quad . \tag{24}$$

Continuity of $F(z)$ and $G(z)$ [or, equivalently, $F'(z)$, in view of Eq. (10)] at $z = 0$, z_0, z_1, z_2, z_3, and L gives rise to 12 equations for the 13 amplitudes and, hence, the two ratios of interest (for each wave), $R = c^{(2)}/c^{(1)}$ and $T = c^{(13)}/c^{(1)}$,

$$R = \frac{-Q^= Q^\pm + \gamma^2 Q^\mp Q^\ddagger}{(Q^\pm)^2 - \gamma^2\left(Q^\ddagger\right)^2} \quad , \tag{25}$$

$$T = \frac{16 K_1 \gamma \Psi^2 \Phi^2 \exp(in_0 L)}{\pi^2\left[(Q^\pm)^2 - \gamma^2\left(Q^\ddagger\right)^2\right]} \quad , \qquad \gamma = \exp\left[in_0 K_1 L\left(1 - \frac{2z_1}{L}\right)\right] \quad , \tag{26}$$

$$Q^{(\pm)}_{(\pm)} = \begin{vmatrix} A^\pm(\Phi) & P_1 & P_3 \\ 0 & A^\pm(\Psi K_1/K_0) & B^\pm(\Psi K_1/K_0) \\ B^\pm(\Phi) & P_2 & P_4 \end{vmatrix} \quad ,$$

where the upper sign on Q identifies the sign on both terms in the first column while the lower sign fixes the sign on both terms in the second row, and

$$P_1 = \begin{vmatrix} A^+(\Psi) & A^-(\Psi) \\ A^+(\Phi K_0) & A^-(\Phi K_0) \end{vmatrix} \quad , \quad P_2 = \begin{vmatrix} A^+(\Psi) & A^-(\Psi) \\ B^+(\Phi K_0) & B^-(\Phi K_0) \end{vmatrix} \quad ,$$

$$P_3 = \begin{vmatrix} B^+(\Psi) & B^-(\Psi) \\ A^+(\Phi K_0) & A^-(\Phi K_0) \end{vmatrix} \quad , \quad P_4 = \begin{vmatrix} B^+(\Psi) & B^-(\Psi) \\ B^+(\Phi K_0) & B^-(\Phi K_0) \end{vmatrix} \quad .$$

The basic composite functions in the solution are, for any argument β,

$$A^\pm(\beta) = a\,i'(\beta^2) \pm \beta a\,i(\beta^2)$$

$$B^\pm(\beta) = b\,i'(\beta^2) \pm \beta b\,i(\beta^2) \quad , \tag{27}$$

and the arguments are of the form,

$$\Phi = -i\left(\frac{n_0 z_0}{m X_0}\right)^{1/3} \quad , \quad \Psi = -iK_0\left[\frac{n_0(z_1 - z_0)}{m(X_1 - X_0)}\right]^{1/3} \quad . \tag{28}$$

The ratios of the reflected and transmitted energy to the incident energy,

$$\epsilon_R = \frac{1}{2}\left(|R_r|^2 + |R_\ell|^2\right) \quad , \tag{29}$$

$$\epsilon_T = \frac{1}{2}\left(|T_r|^2 + |T_\ell|^2\right) \quad , \tag{30}$$

-10-

were computed in a parametric fashion from the solutions (25) and (26). The incident wave ($z < 0$) is now assumed to be linearly polarized, say along the x-axis (E_x and H_y components only), so that the amplitude $c^{(1)}$ is the same for the left- and right-hand waves. The principal effect of interest is that of the inhomogeneity which manifests itself through two independent quantities, namely, the transition distance and the profile details. The ratio of transition distance to slab thickness has the values $0 \le z_1/L \le 0.5$, in the present problem, while 16 separate profiles are assumed as determined by the location of the kink and its ordinate, i.e., $z_0/z_1 = 0.2, 0.4, 0.6, 0.8$, and $X_0/X_1 = 0.2, 0.4, 0.6, 0.8$. This effect is demonstrated by plotting the degradation in transmitted energy $db_T = 10 \log_{10} \epsilon_T$, normalized with respect to the corresponding homogeneous plasma slab value ($z_1/L = 0$), versus z_1/L for the extreme cases $X_0/X_1 = 0.2$, $z_0/z_1 = 0.8$ and $X_0/X_1 = 0.8$, $z_0/z_1 = 0.2$, as well as for the straight trapezoidal profile $X_0/X_1 = z_0/z_1$. Only numerical results for transmission are presented in this report.

It is immediately apparent that the transmission through an inhomogeneous plasma slab can be substantially greater than the corresponding value for the homogeneous slab. Both the transition distance and the profile details can significantly reflect this effect. Thus, in Fig. 2a ($Z = 1$), for example, when $z_1/L = 0.5$, transmission is increased by 21 percent over the corresponding homogeneous plasma result for $X_0/X_1 = 0.8$, $z_0/z_1 = 0.2$ and by 83 percent for $X_0/X_1 = 0.2$, $z_0/z_1 = 0.8$. In the latter case, a 10 percent increase is shown for an order of magnitude smaller value of $z_1/L = 0.05$. A qualitative appreciation for what is involved can be obtained from the assumed distribution of $X(z)$ shown in Fig. 1. In particular, one would expect to improve transmission, in general, when the plasma is made less dense relative to the homogeneous case. This is essentially what is done when z_1/L is increased (for fixed values of X_1, Z, and L/λ_0) or when the assumed profile is altered by decreasing X_0/X_1 or increasing z_0/z_1. The accuracy of a homogeneous plasma slab analysis will improve as the distribution of $X(z)$ approaches the constant value X_1.

Clearly, transmission also depends on the reference parameters X_1, Z, Y, and L/λ_0. For the same conditions noted above, for example, a value of Z = 0.01 results in increases in transmission of 31 percent and 96 percent, respectively. The influence of Z in this figure is even more substantial for the trapezoidal profile. Parametric calculations were made for L/λ_0 = 0.5 and 1.0 including moderately overdense conditions (i.e., $1 < X_1 \leq 4$), comparable values of $0 \leq Y \leq 3$ required to improve transmission to the level of practical interest, and $0.01 \leq Z \leq 1$. Illustrative results are shown in Figs. 2a through 2k. Estimates can be made in any particular application with this series of graphs. Additional calculations would be required if the conditions of interest are too far removed from these values. This situation will be considered further in the analyses of Sections III. B and IV as noted in the following paragraph.

Several curves in Figs. 2f and 2g are incomplete in that the results are not shown for the larger values of z_1/L, which calls attention to the fact that the computations using Eq. (26) met with numerical difficulties when the magnitude of any of the arguments Φ, Ψ, ΦK_0, or $\Psi K_1/K_0$ became large. This difficulty not only precluded the aforementioned calculations at z_1/L = 0.5 but also prevented the desirable extension of our parametric analysis to larger values of X_1 and Y, as well as L/λ_0. Since highly overdense plasmas are encountered in a number of applications, in which case values of Y of comparable size would be required to make the applied magnetic field effective, it is desirable to consider the range X_1, Y >> 1. This information is derived from the analysis of the next section.

It should be remarked that in the cases where at least one argument becomes too large for our calculation procedure, the conditions of interest at L/λ_0 = 0.5 and 1.0 are such that one or more of the remaining arguments may still be relatively small, thereby forestalling any general asymptotic analysis. An asymptotic expansion of the exact solution is derived below, however, to provide information for larger values of L/λ_0. In this regard, note that expansions of any solution for large (or small) values of more than

one independent quantity in any problem are meaningful only when proper consideration is given to their order of magnitude relative to each other as well as relative to the number one. This formal observation becomes of practical interest in the proper use of the resultant simplified expressions for computational purposes. The small L/λ_0 limit will be examined separately in Section IV.

Using the asymptotic representation of the Airy function, we obtain

$$A^{\pm}(\beta) = \frac{1}{2\sqrt{\pi}}\beta^{1/2} \exp\left(-\frac{2}{3}\beta^3\right)\left(a_0^{\pm} + a_1^{\pm}\beta^{-3} + a_2^{\pm}\beta^{-6} + a_3^{\pm}\beta^{-9} + \cdots\right) \quad ,$$

$$B^{\pm}(\beta) = \frac{1}{\sqrt{\pi}}\beta^{1/2} \exp\left(\frac{2}{3}\beta^3\right)\left(b_0^{\pm} + b_1^{\pm}\beta^{-3} + b_2^{\pm}\beta^{-6} + b_3^{\pm}\beta^{-9} + \cdots\right) \quad ,$$

for $-\pi < \arg\beta < \pi$, where

$$a_0^{\pm} = -1 \pm 1 \quad ,$$

$$a_1^{\pm} = -(7 \pm 5)/48 = b_1^{\mp} \quad ,$$

$$a_2^{\pm} = (455 \pm 385)/4608 = -b_2^{\mp} \quad ,$$

$$a_3^{\pm} = -(95095 \pm 85085)/663552 = b_3^{\mp} \quad ,$$

$$b_0^{\pm} = 1 \pm 1 \quad .$$

-13-

The expansion ceases to be valid when

$$\theta = \frac{3\pi}{2} - 2k\pi \qquad \text{or} \qquad \theta + 3 \arg K_0 = \frac{3\pi}{2} - 2k\pi \quad , \qquad k = 0, 1, 2, \cdots \quad ,$$

where $\theta = -\tan^{-1} Z/M$; and convergence will be poor in the vicinity of these conditions. The general asymptotic expansion of (25) and (26) for arbitrary, large values of the parameters becomes

$$R \sim \frac{\gamma^2 (S_1 \bar{S}_3 - S_3 \bar{S}_1)[S_4 \bar{S}_3 + (1/64)S_2 S_1] + (S_2 \bar{S}_4 - S_4 \bar{S}_2)[S_3 \bar{S}_4 + (1/64)S_1 \bar{S}_2]}{8[S_3 \bar{S}_4 + (1/64)S_1 \bar{S}_2]^2 - (\gamma^2/8)(S_1 \bar{S}_3 - S_3 \bar{S}_1)^2} \tag{31}$$

$$T \sim \frac{\gamma \exp(in_0 L)}{[S_3 \bar{S}_4 + (1/64)S_1 \bar{S}_2]^2 - (\gamma^2/64)(S_1 \bar{S}_3 - S_3 \bar{S}_1)^2} \quad , \tag{32}$$

where

$$S_1 = V_-(\Phi)V_+(\Phi K_0)\mathcal{E}^- - V_-(\Phi K_0)V_+(\Phi)\mathcal{E}^+ \quad ,$$

$$S_2 = W_-(\Phi K_0)W_+(\Phi)\mathcal{E}^+ - W_-(\Phi)W_+(\Phi K_0)\mathcal{E}^- \quad ,$$

$$S_3 = W_-(\Phi K_0)V_+(\Phi)\mathcal{E}^+ + \frac{1}{64}V_-(\Phi)W_+(\Phi K_0)\mathcal{E}^- \quad ,$$

$$S_4 = W_-(\Phi)V_+(\Phi K_0)\mathcal{E}^- + \frac{1}{64}V_-(\Phi K_0)W_+(\Phi)\mathcal{E}^+ \quad ,$$

$$\mathcal{E}^\pm = \exp\left\{\pm\frac{2}{3}\left[\Phi^3 - (\Phi K_0)^3\right]\right\} \quad ;$$

the $\bar{S}_i$ functions are obtained upon replacing Φ by $\Psi K_1 / K_0$, replacing ΦK_0 by Ψ (for each $i = 1, 2, 3, 4$), and, for any argument β,

$$V_\mp = \left(\mp \beta^{-3} + \frac{105}{144} \beta^{-6} \mp \frac{45045}{41472} \beta^{-9} + \cdots \right) \quad ,$$

$$W_\mp = \left(\mp 1 - \frac{1}{48} \beta^{-3} \pm \frac{35}{4608} \beta^{-6} - \frac{5005}{663552} \beta^{-9} + \cdots \right) \quad .$$

This result may be used for calculation purposes, keeping track of the relative magnitudes of all four arguments and the correct number of terms which therefore must be included. Retaining only the leading terms in the expansion, we obtain the following limiting expression for the transmission coefficient:

$$T \sim \gamma \, \exp(in_0 L) \, \exp\left(-\frac{4}{3}\right) \left[\Phi^3 \left(1 - K_0^3\right) + \Psi^3 \left(1 - \frac{K_1^3}{K_0^3}\right) \right] \quad , \tag{33}$$

which, for the special case of a straight trapezoidal profile

$$\Psi \to \Phi K_0 \quad , \qquad \Phi \to -i \left(\frac{n_0 z_1}{m X_1}\right)^{1/3} \quad ,$$

reduces to the simplified, useful expression

$$T \sim \gamma \, \exp(in_0 L) \, \exp\left(-\frac{4}{3}\right) \left[\Phi^3 - (\Phi K_1)^3 \right]$$

$$= \gamma \, \exp(in_0 L) \, \exp\left[-\frac{4 i n_0 z_1}{3} \left(1 + \frac{K_1^2}{1 + K_1}\right) \right] \quad . \tag{34}$$

The convergence of (32) is such that Eqs. (33) and (34) can be used to compute transmission when the magnitude of the arguments is greater than two. The corresponding values of L/λ_0 would depend on the conditions involved and may be as small as one in a number of cases of interest. Although (34) is particularly useful for this purpose because of its relative simplicity, it is limited to profiles which are approximately trapezoidal. Additional flexibility is provided by (33) which includes an arbitrary kink in the linear representation of the inhomogeneous region. In both cases, the accuracy of the calculation can be improved, or a smaller value of L/λ_0 can be considered for a given set of conditions, by including additional terms from the general expansion (32).

A homogeneous plasma slab geometry was used in Ref. 2 to estimate the increase in transmission resulting from an applied magnetic field for several exemplary re-entry situations. One case considered was that of a 10 degree cone at zero angle of attack for a variety of flight conditions. In the present work, calculations have been made for the same conditions using the inhomogeneous profile shown in Fig. 3. This is a special case of the general problem that is treated in this section, which can be shown to be a reasonable approximation to the present flight application. A comparison between the more realistic inhomogeneous plasma values and the previously obtained results for a homogeneous plasma is shown in Figs. 4a through 4c. To discuss the effect of a magnetic field in eliminating "blackout," we must establish a reference level of acceptable transmission. Since this value is often difficult to ascertain, even for current applications which are well along in the development phase, it will be necessary to base our remarks on several possible assumed values.

Consider first the telemetry frequency (f = 240 Mc) and lower re-entry velocity given in Fig. 4b. If 10-db degradation in transmitted energy is acceptable, no magnetic field is required because the possibly marginal maximum homogeneous value of 9.75 db at 150,000 ft (B_0 = 0) is now replaced by the corresponding inhomogeneous value of 6.1 db. If, however, a

maximum of 5 db is allowed, then blackout should occur at 150,000 ft. Moreover, although a magnetic field strength of 250 gauss would have to be applied to reduce the homogeneous prediction to 5 db, only 50 gauss is required to attain this figure using the more realistic inhomogeneous plasma calculations. The more severe re-entry condition with u = 26,000 fps is shown in Fig. 4a (f = 240 Mc). Although the 150,000-ft condition is still more critical than 100,000 ft with no magnetic field, we should note the particularly strong dependence of db_T on the applied magnetic field in the former case. Referring now to inhomogeneous plasma results alone, we see that there is no transmission problem at 100,000 ft if 15 db is acceptable 250 gauss is needed to eliminate blackout at 150,000 ft. For 10 db, 650 gaus would be required at 150,000 ft, while 1350 gauss would be needed at 100,00(ft. At the 5 db-level, the sharply reduced effect of B_0 for 100,000 ft makes this condition even more critical. Indeed 4200 gauss would be needed to avoid blackout in the former, while 1300 gauss would be enough in the latter case. A qualitatively similar situation is shown in Fig. 4c when $f = 3 \times 10^9$ cps (u = 26,000 fps).

The assumption of a homogeneous plasma slab is severely pessimistic for the re-entry cone application. It is of interest that transmission is due primarily to a skin depth effect. In particular, for f = 240 Mc and u = 26,000 fps, the fact that the plasma is highly overdense (Fig. 3) is offset by the correspondingly small values of L/λ_0 involved. The determination of transmission for each flight condition is greatly dependent on this effect[2] whether the plasma is homogeneous or inhomogeneous. The influence of the magnetic field on transmission is also dependent on this situation since it is generally more pronounced when the level of X is lower.[1] This accounts for the abrupt variation of db_T with B_0 at 150,000 ft (Fig. 4a) in contrast with the sharply reduced effect at 50,000 ft where X_1 is an order of magnitude larger. The combined effect of all of these quantities is shown in Figs. 4a through 4c and the results are discussed in the preceding paragraph for both the homogeneous and more realistic inhomogeneous plasma models.

B. Exponential-Homogeneous-Exponential Electron Density Distribution

The analysis of the preceding boundary value problem provided a clear indication of the significant influence of plasma inhomogeneities on propagation for a range of conditions of interest. Detailed numerical results can be obtained for specific problems also, approximating the actual electron density distribution by the assumed profile (Fig. 1), as was done in the evaluation of a re-entering cone. It is desirable for several reasons to consider yet another formal inhomogeneous plasma slab problem. The need to extend the range of conditions previously considered to include larger values of X_1 and $\cdot$ has already been noted. The present results are also of importance in the small L/λ_0 analysis of Section IV. Therefore, let us examine the formal solution of Eq. (11) for the following assumed profile (see Fig. 5):

$$
\left.
\begin{aligned}
X(z) &= 0 \quad , \quad z \leq 0 \quad , \\
&= X_\infty(1 - e^{-az}) \quad , \quad a > 0 \quad , \quad 0 \leq z \leq z_1 \quad , \\
&= X_\infty\left(1 - e^{-az_1}\right) \quad , \quad z_1 \leq z \leq z_2 \quad , \quad (z_2 = L - z_1) \\
&= X_\infty[1 - e^{-a(L-z)}] \quad , \quad z_2 \leq z \leq L \quad , \\
&= 0 \quad , \quad z \geq L \quad .
\end{aligned}
\right\} \quad (35)
$$

The solutions in the several regions are as follows.

For $z \leq 0$:

$$
F(z) = c^{(1)} e^{-in_0 z} + c^{(2)} e^{in_0 z} \quad . \tag{36}
$$

For $0 \leq z \leq z_1$, Eq. (11) becomes:

$$
F'' + n_0^2\left[1 - mX_\infty(1 - e^{-az})\right]F = 0 \quad .
$$

-18-

Introducing the change of independent variables

$$\bar{\xi} = \frac{2n_0}{a}(mX_\infty)^{1/2} e^{-az/2} \quad , \tag{37}$$

where $m^{1/2}$ is chosen so that its imaginary part is positive, we obtain Bessel's equation

$$\frac{d^2F}{d\bar{\xi}^2} + \frac{1}{\bar{\xi}}\frac{dF}{d\bar{\xi}} + \left(1 - \frac{\alpha^2}{\bar{\xi}^2}\right)F = 0 \quad , \qquad \alpha = \frac{2in_0}{a}(1 - mX_\infty)^{1/2} \tag{38a}$$

and, therefore, a general solution ($\alpha \neq$ integer) in terms of Bessel functions

$$F(\bar{\xi}) = c^{(3)}J_\alpha(\bar{\xi}) + c^{(4)}J_{-\alpha}(\bar{\xi}) \quad . \tag{38b}$$

For $z_1 \leq z \leq z_2$:

$$F(z) = c^{(5)} \exp(in_0)\left[1 - mX_\infty\left(1 - e^{-az_1}\right)\right]^{1/2}$$

$$+ c^{(6)} \exp(-in_0)\left[1 - mX_\infty\left(1 - e^{-az_1}\right)\right]^{1/2} \tag{39}$$

while for $z_2 \leq z \leq L$ and $z \geq L$, respectively,

$$F(\bar{\eta}) = c^{(7)}J_\alpha(\bar{\eta}) + c^{(8)}J_{-\alpha}(\bar{\eta}) \quad , \tag{40}$$

$$\bar{\eta} = \frac{2n_0}{a}(mX_\infty)^{1/2} \exp\left[-\frac{a}{2}(L - z)\right] \quad , \tag{41}$$

$$F(z) = c^{(9)} e^{-in_0 z} \quad . \tag{42}$$

-19-

Continuity of $F(z)$ and $F'(z)$ at $z = 0$, z_1, z_2, and L gives rise to eight equations for the nine amplitudes and, hence, the two ratios of interest (for each wave)

$$R = \frac{(D^-M^+ - C^-N^+)(C^+N^+ - D^+M^+) - \gamma^2(D^-M^- - C^-N^-)(C^+N^- - D^+M^-)}{(D^-M^+ - C^-N^+)^2 - \gamma^2(D^-M^- - C^-N^-)^2} \quad , \quad (43)$$

$$T = \frac{-4\psi\gamma\left(a^2/\pi^2 n_0^2\right)\exp(in_0 L)\sin^2 a\pi}{(D^-M^+ - C^-N^+)^2 - \gamma^2(D^-M^- - C^-N^-)^2} \quad , \quad (44)$$

$$C^{\pm} = i(mX_\infty)^{1/2} J'_a(\phi) \pm J_a(\phi) \quad ,$$

$$D^{\pm} = i(mX_\infty)^{1/2} J'_{-a}(\phi) \pm J_{-a}(\phi) \quad ,$$

$$M^{\pm} = (mX_\infty)^{1/2} \exp\left(-\frac{az_1}{2}\right) J'_a\left[\phi \exp\left(-\frac{az_1}{2}\right)\right] \pm i\psi J_a\left[\phi \exp\left(-\frac{az_1}{2}\right)\right] \quad ,$$

$$N^{\pm} = (mX_\infty)^{1/2} \exp\left(-\frac{az_1}{2}\right) J'_{-a}\left[\phi \exp\left(-\frac{az_1}{2}\right)\right] + i\psi J_{-a}\left[\phi \exp\left(-\frac{az_1}{2}\right)\right] \quad ,$$

$$\phi = \frac{2n_0}{a}(mX_\infty)^{1/2} \quad , \quad \psi = (1 - mX_1)^{1/2} \quad , \quad a = \frac{2in_0}{a}(1 - mX_\infty)^{1/2} \quad ,$$

$$\gamma = \exp\left[in_0\psi L\left(1 - \frac{2z_1}{L}\right)\right] \quad , \quad X_1 = X_\infty\left(1 - e^{-az_1}\right) \quad .$$

In the limit as $a \to \infty$, Eqs. (43) and (44) reduce to the well-known homogeneous plasma slab results.[1]

The quantities ϵ_R and ϵ_T [see Eqs. (29) and (30)] were computed, parametrically, from the solutions (43) and (44). In a similar manner to the presentation of the kinked-trapezoid results, the ratio $db_T/(db_T)_0$ is

plotted versus z_1/L in Figs. 6a through 6g for a range of conditions. Four values of $a\lambda_0$ (characterizing the profile shape) were assumed, namely, $a\lambda_0 = 2, 4, 6, 12$, and the range of X_1 and Y was extended to include the values 400 and 100, respectively. Although it was not the purpose of this calculation to compare the two general distributions which have been assumed, such a comparison was made for several typical cases. As expected, the results are the same when the profiles are made approximately coincident. It is also of interest that the results for the exponential geometry approach the trapezoid values when $\underline{a}$ is sufficiently small, as is illustrated graphically in Fig. 6a.

A wide range of detailed profiles (exponential and kinked-trapezoidal in character) and values of X_1, Z, and Y has now been examined, parametrically, for $L/\lambda_0 = 0.5$ and, to a lesser extent, $L/\lambda_0 = 1$. The resultant series of illustrative graphs which are included in this report can be used to effectively estimate transmission for particular problems of interest, the principal restriction in coverage being the two values of L/λ_0 assumed. Approximate calculations can be made readily, however, for larger values of L/λ_0 using the simplified Eq. (34) or, if necessary, (33) or (32). In the next section, a basic and particularly useful result is established for the small L/λ_0 regime. The present consideration of a second class of profiles provided the additional numerical foundation of an exact analysis which was essential in the verification of this result.

SECTION IV

PROPAGATION ACROSS THIN INHOMOGENEOUS PLASMA SLABS:[*] SMALL L/λ_0

One of the more apparent deficiencies in the extent of quantitative information presented in Section III lies in the limited consideration given to small values of L/λ_0. In the present section, we will examine in detail the propagation problem when $L/\lambda_0 \ll 1$. The desire to merely extend the coverage in numerical information which could be partially accomplished using a small argument expansion of the exact solutions led to the verification of a rather basic and particularly useful result. In this regard, it is of interest to recall our previously mentioned treatment of the re-entry cone problem. All of the conditions shown in Fig. 3 are in the small L/λ_0 range, even for the higher frequency of $f = 3 \times 10^9$ cps. Indeed, it has been observed that this so-called skin depth effect is what makes transmission possible even when the plasma is highly overdense.

The present discussion will be based primarily upon the use of the exact solutions derived in the preceding section. The following limiting situation is offered to advance the necessary initial insight. It should be emphasized that this calculation is intended to serve as a guide in the proper use of our exact solutions of the full wave equations; no formal investigation of the problem is intended along these lines.

Consider propagation across a vanishingly thin plasma sheath separating two free space regions as described in Section II. In the free space regions, $z < 0$ and $z > L$, respectively,

$$F_1 = c^{(1)} e^{-in_0 z} + c^{(2)} e^{in_0 z} \quad , \tag{45}$$

$$F_3 = c^{(3)} e^{-in_0 z} \quad . \tag{46}$$

The two waves propagating in the plasma ($0 < z < L$) satisfy the equation

$$F_2'' + n_0^2 [1 - mX(z)] F_2 = 0 \quad . \tag{47}$$

We would like to consider the limiting case of $L \to 0$, $X \to \infty$ (i.e., the maximum value in the layer). Let us, therefore, represent the function $X(z)$ by a Dirac delta function at $z = 0$, $\delta(z)$,

$$X(z) = (\overline{X}L)\delta(z) \quad , \qquad \overline{X}L = \int_0^L X(z)dz \quad . \tag{48}$$

Substituting this into (47), we obtain

$$F_2'' + n_0^2 F_2 - n_0^2 m\overline{X}L\delta(z)F_2 = 0 \quad . \tag{49}$$

Integrating from zero to z, we see that

$$F_2' = (F_2')_0 + n_0^2 m\overline{X}L(F_2)_0 \quad , \tag{50}$$

where the contribution of $n_0^2 F_2$ in (49) is zero in the present limit since F_2 is assumed to be continuous, and the subscript zero denotes the value at $z = 0$. For $L \to 0$, therefore, F_2' (or the magnetic field) has a simple discontinuity, and when the boundary conditions are applied we obtain the following results:

$$R = \frac{-m\overline{X}n_0 L}{2i + m\overline{X}n_0 L} \quad , \tag{51}$$

$$T = 1 + R = \frac{1}{1 - (in_0 L/2)m\overline{X}} \quad , \qquad (52)$$

$$\frac{(F_2)_0}{c^{(1)}} = \frac{(F_2)_L}{c^{(1)}} = T \quad , \qquad \frac{(F_2')_L}{c^{(1)}} = -in_0 T \quad , \qquad \frac{(F_2')_0}{c^{(1)}} = -in_0(1 - R) \quad . \qquad (53)$$

Evaluating the Poynting vector, we obtain

$$\epsilon_T = \frac{1}{2}\left(|T_r|^2 + |T_\ell|^2\right)$$

$$(54)$$

$$= \frac{1}{2}\left\{\frac{M_r^2 + z^2}{M_r^2 + [z + (\pi L/\lambda_0)\overline{X}]^2} + \frac{M_\ell^2 + z^2}{M_\ell^2 + [z + (\pi L/\lambda_0)\overline{X}]^2}\right\} \quad ,$$

where $M_r = 1 - Y$, $M_\ell = 1 + Y$. (Two related problems of considerable interest are briefly analyzed in the Appendix using a similar approach.)

We should like now to suggest that the problem of propagation across a plasma slab in which the ratio L/λ_0 is small, $X(z)$ is arbitrary, and the maximum value of X is large, is not dependent upon the details of the electron density distribution but only on the integrated value across the slab. Although this assumption is made in the analysis of radio waves from meteor trails, for example, [3] and in a number of related problems in classical physics, it is our intention to verify it using the exact solutions previously obtained in Section III. As a consequence, a considerable simplification in the analysis of specific propagation problems of this type is obtained.

An obvious deduction from the preceding remarks is that an approximate solution to the aforementioned problem can be obtained from the consideration of a homogeneous slab having the same width L and an equivalent value of $\overline{X}$ determined from the relation

$$\overline{X}L = \int_0^L X(z)\,dz \quad , \qquad (55)$$

where $X(z)$ is the known distribution. For the exponential profile treated in Section III. B, therefore,

$$\frac{X}{X_1} = 1 - 2 \frac{z_1}{L} \left[1 - \frac{1}{1 - \exp(-az_1)} + \frac{1}{az_1} \right] \quad , \tag{56}$$

and, for the kinked-trapezoid,

$$\frac{X}{X_1} = 1 - \frac{z_1}{L} \left(1 - \frac{X_0}{X_1} + \frac{z_0}{z_1} \right) \quad . \tag{57}$$

Therefore, the transmission coefficient can be determined using the corresponding equivalent index of refraction, $\bar{n}^* = (1 - m\bar{X})^{1/2}$

$$T = \frac{4\bar{n}^* \exp(in_0 L)}{(\bar{n}^* + 1)^2 \exp(in_0\bar{n}^*L) - (\bar{n}^* - 1)^2 \exp(-in_0\bar{n}^*L)} \quad . \tag{58}$$

It is interesting to note that Eq. (52) follows from (58) when the magnitude of $in_0\bar{n}^*L$ is small (retaining only the leading term in the expansion and using the assumption of small L/λ_0, large X, to further simplify). The basic premise that propagation is principally dependent on the integrated value of $X(z)$ when $L/\lambda_0 \ll 1$ will now be examined by comparing the results of the approximate and the exact solutions. This conclusion is of considerable importance in many propagation studies. The practical value of using (52) or even (58) to compute transmission (or reflection, from the related expressions) for an arbitrary $X(z)$ in the present problem is evident. The following correlation will also be used, therefore, to determine the range of conditions for which approximate calculations can be made on this basis.

The transmission coefficient has been computed from the exact solution (44) for the three typical exponential profiles shown in Fig. 7, covering the following range of conditions:

L/λ_0	X_1	Z	Y
0.001	100, 1000, 10000	10, 100	0, 100
0.01	25, 100, 1000	1, 10, 100	0, 10
0.1	2.25, 25, 100, 400	0.01, 1, 10	0, 5, 100 .

An equivalent homogeneous plasma was determined using Eq. (56) and T was computed from (58). The equivalent homogeneous plasma results for $L/\lambda_0 = 0.001$ and 0.01 are virtually identical to the exact values, indeed $(db_T)_{exact}/(db_T)_{\overline{X}} = 1.00$, for all cases considered. Complete agreement gives way to more than acceptable correlation for most applications when L/λ_0 is increased to 0.1. All three profiles and a wide range of conditions were included in these calculations in order to examine the applicability of our approximate analysis. Less than three-percent error was found in the computations involving profile I. Although the homogeneous plasma values of db_T for $X = X_1$ are already close to the exact results (within 10 percent), as would be expected for this profile, the additional accuracy obtained using $X = \overline{X}$ is noteworthy in many applications. The discrepancy increased in general, to a maximum of five percent, for profile II which differs even further from the constant $X = X_1$ distribution. The maximum discrepancy noted in the 36 cases considered for profile III (which is now substantially different than $X = X_1$) was only seven percent. In general, even greater accuracy is obtained, for each assumed profile, as X_1 is decreased, for fixed Z, or as Z is increased, for fixed X_1.

In the preceding correlation, we established the basic premise that the propagation is dependent on $\overline{X}$ and began to determine limiting conditions under which the resultant convenient calculation procedure can be used. Consistent with the approach outlined at the outset of this section, we will

not attempt to derive a formal limiting criterion. Although this would be desirable and may be examined using several different expansion procedures suggested by the problem, the present purpose is best accomplished by continuing to use the same procedure. The exact solutions, therefore, will now be used to provide the required empirical limiting information.

Only a relatively few calculations were made for $L/\lambda_0 = 0.5$ using the exponential profile, in particular $X_1 = 1.21$, 2.25, 25; $Z = 0.01$, 1; and $Y = 0$. It is first apparent (for the extreme profile III) that agreement is poor, in percentage, when $Z = 0.01$, $X_1 = 1.21$. In addition, although a comparison with the corresponding $L/\lambda_0 = 0.1$ results shows an expected decrease in accuracy, the maximum error for the remaining conditions of interest is still only seven percent. It will be convenient to use the analysis of Section III. A to examine these two points further. Transmission coefficients were obtained from the exact solution (26) for the range of kinked-trapezoid profiles shown in Fig. 8 and the conditions

$$X_1 = 1.44, \ 2.25, \ 4; \quad Z = 0.01, \ 1; \quad Y = 0, \ 0.5, \ 1.5, \ 3 \quad .$$

Using Eq. (57), we obtain for the equivalent homogeneous plasma slab, $\overline{X}/X_1 = 0.5(1 + X_0/X_1 - z_0/z_1)$. The results are tabulated in Fig. 9. For $Y = 0$, $Z = 1$ less than three-percent error was obtained (for all profiles) at $X_1 = 1.44$ and 2.25, and less than seven percent at $X_1 = 4$. By contrast, the correlation experiences some difficulties for $Z = 0.01$. The accuracy is generally improved as X_1 is increased (depending on the profile), particularly for $Z = 0.01$; indeed the error obtained at $X_1 = 4$, $Z = 0.01$, now ranges from one to 13 percent for all cases (except one). At the same time, note also that for a fixed value of X_1 there is a marked improvement in the correlation when either X_0/X_1 is increased with z_0/z_1 held fixed or z_0/z_1 is decreased with X_0/X_1 fixed. The principal factor involved appears to be the abrupt dependence of ϵ_T on X near the resonant condition when Z is small. Part of the plasma is always overdense because we have assumed $X_1 > 1$. A smaller

value of X_0/X_1 and/or a larger value of z_0/z_1 will reduce the ratio $\bar{X}/X_1$, the minimum value being 0.2 for the profiles considered. In this case, for $X_1 = 1.44$, $\bar{X} = 0.288$ and the equivalent homogeneous plasma will not include any resonant effect. Although the percentage error is large in this case, it is interesting to observe that the magnitude of db_T is quite small which therefore may be more of academic than practical concern.

At the other extreme, $\bar{X} = 1.152$, the resonant condition is more accurately taken into account, and an error of only 12 percent is obtained. Note the magnitude of db_T involved. As X_1 is increased, the region in which X is of order one represents a smaller portion of the total distribution. Its effect on transmission will be reduced, and a qualitatively similar but substantially improved correlation is shown for $X_1 = 2.25$. As was previously noted, the over-all agreement is quite good when $X_1 = 4$. The major effect described above is still evident since for the extreme profile when $\bar{X} = 0.8$ the percentage error is sizable, whereas good agreement is obtained in all of the remaining cases since the equivalent value of $\bar{X}$ is further from the resonant value. The maximum discrepancy is less than seven percent at $Z = 1$ for all cases including a magnetic field. The way in which X_1 and Y combine to effect the correlation may be seen from the detailed results given in Fig. 9. The presence of a magnetic field modifies the preceding discussion for $Z = 0.01$ in certain instances. Although the qualitative conclusions often apply, it is best to refer to the detailed correlation to evaluate the prospective accuracy of the approximate procedure for a specific combination of X_1 and Y of interest.

The following conclusions can be made in summary. Using the exact solutions derived earlier in this report, we have shown that the transmission across a thin $(L/\lambda_0 \ll 1)$ inhomogeneous plasma sheath depends on the total integrated value of electron density, not on the detailed distribution. Such an assumption is often the essential starting point for investigations of propagation in this limit and is of particular value in the present analysis. Accurate transmission calculations can be made on this basis for $L/\lambda_0 \leq 0.1$ using the

considerably simplified homogeneous plasma slab expression (58) and an
equivalent constant value of X determined from (55). Indeed for the broad
range of conditions considered in establishing this fact, there is virtually
complete agreement between the exact and the approximate results for
L/λ_0 = 0.001 and 0.01. When L/λ_0 was increased to 0.1, the maximum
discrepancy found in the computations for 108 different cases (including
three profiles), covering the full spectrum of transmission levels of possible
interest, was only seven percent. In general, even greater accuracy is
obtained when the profile approaches the constant $X = X_1$ distribution or, for
an assumed profile, when either X_1 is decreased or Z is increased. For
L/λ_0 = 0.5, smaller values of X_1, Z, and Y were used, along with a number
of profiles, and a maximum error of seven percent was obtained when Z = 1.
The correlation at Z = 0.01 was substantially affected by the values of X_1
and Y and by the profile. Although the previous discussion for Y = 0 is
informative, it is best to refer to the detailed results of Fig. 9 to evaluate
a particular condition of interest.

It should be remarked that we have not attempted rigorously to determine
a formal limiting condition for the approximate calculation procedure. Although
its accuracy (better than 93 percent) was established in detail, in an empirical
manner for virtually any condition of practical interest, even when L/λ_0 = 0.1,
only limited calculations were made for larger values of L/λ_0 where the
procedure will begin to fail. However, for L/λ_0 = 0.5 (and, to a lesser extent,
L/λ_0 = 1) transmission can be adequately determined from the detailed con-
siderations of Section III which includes a large measure of arbitrariness in
the assumed distribution of X(z) and a broad parametric treatment of the
remaining quantities. The evaluation of our appproximate procedure at
L/λ_0 = 0.5 is intended to complement these results when calculations are
required for intermediate values of the parameters or for transitional values
of L/λ_0, say between 0.1 and 1.0. We shall now illustrate the way in which
the two procedures can be used to complement one another. Recall that accu-
rate results (less than seven-percent error) were obtained from the approxi-
mate calculations at L/λ_0 = 0.5 when Z = 1. Thus, transmission results can be

computed at $Z = 1$ for the intermediate values of X_1 which are not included in the graphs obtained in Section III. A. Estimates also can be made on this basis for values of Z which are close to one, covering the entire range of X_1 considered. On the other hand, the dependence on Z shown in these graphs can be used to estimate transmission when Z is small, aided to some extent by an approximate calculation whose accuracy can be evaluated from Fig. 9.

A vivid demonstration of the obvious utility of the simplified small L/λ_0 expressions follows. A triangular distribution of $X(z)$ was previously assumed to represent the plasma about a re-entry cone (Fig. 3). With the aid of a high-speed computer, the exact solution derived in Section III. A was used, therefore, to calculate transmission. The results obtained when $f = 240$ Mc can be easily reproduced (within several percent) using the limiting algebraic expression (54). Satisfactory agreement was not obtained at $f = 3,000$ Mc when (54) was no longer appropriate, i. e., for conditions where the magnitude of $in_0 \bar{n}*L$ is not small. Excellent agreement with the exact calculations was obtained in all cases using Eq. (58). It follows from the general correlation of (58) with the exact solutions of Section III that (54) may be used to simplify computations even further, when applicable. It is perhaps redundant to add that homogeneous plasma slab calculations can be obtained, in general, from (54) rather than from the more complicated (58) when $|in_0 n*L|$ is small. The result may still be substantially less than perfect transmission in this situation since a small value of $n_0 L$ may be offset by a correspondingly large value of $|\bar{n}*|$ with the product still remaining less than one.

SECTION V

CONCLUSIONS

Exact solutions for the reflection and transmission coefficients have been obtained for several exemplary transition zones between dielectric and dissipative gases. Normal incidence into a stratified plasma slab is assumed so that the electromagnetic waves are propagating parallel to the free electron density gradients. The magnetic field is constant and is applied in the propagation direction. Two general electron density distributions are considered in which both the shape and the extent of the inhomogeneous profile may be varied.

    (i)   Kinked-trapezoid (Fig. 1),

    (ii)   Exponential-homogeneous-exponential (Fig. 5).

The solutions derived on this basis are used to evaluate the effect of an inhomogeneous plasma on electromagnetic wave propagation, parametrically, both with and without an applied magnetic field. At the same time, previously[2] obtained homogeneous plasma calculations for a re-entry cone are refined using the analysis of problem (i).

The kinked-trapezoid geometry is considered in Section III. A, and the resultant expressions for the reflection and transmission coefficients are given by Eqs. (25) and (26), respectively. Parametric calculations were made for $L/\lambda_0 = 0.5$, 1.0 including moderately overdense plasmas, i.e., $1 < X_1 \leq 4$, comparable values of $0 \leq Y \leq 3$ required to improve transmission to the level of practical interest, and $0.01 \leq Z \leq 1$. Illustrative results for db_T, normalized by the corresponding homogeneous value are shown in Figs. 2a through 2k varying the details of the assumed profile.

The second general profile was examined in Section III. B with the solutions given by Eqs. (43) and (44). The resultant calculations for $L/\lambda_0 = 0.5$, 1.0, including larger values of X_1 and Y, are illustrated in a similar manner in Figs. 6a through 6g. The wide range of detailed profiles

(exponential and kinked-trapezoidal in character) and values of X_1, Z, Y covered in the two sets of graphs can be used to estimate transmission, the principal restriction being the two values of L/λ_0 assumed.

Transmission calculations for larger values of L/λ_0 can be directly obtained from the asymptotic expansion of Eq. (26). The resultant limiting expressions (34) and (33) are applicable for values of L/λ_0 as small as one, depending on the conditions involved, due to the rapid convergence of (32) when the magnitude of the arguments is of the order of two. Although (34) is particularly useful for this purpose because of its relative simplicity, it is limited to profiles which are approximately trapezoidal; additional flexibility is provided by (33) which includes a kink in the profile. In both cases the accuracy of the calculation can be improved, or a smaller value of L/λ_0 can be considered for a given set of conditions, by including additional terms from the general expansion (32).

The detailed exact solutions of problems (i) and (ii) were used for yet another purpose in the analysis of Section IV. In that section the problem of propagation across thin inhomogeneous plasma slabs was treated. Numerical calculations using these exact solutions were the principal means of verifying the resultant small L/λ_0 analysis. A brief consideration of the limiting problem of a vanishingly thin plasma sheath ($L \to 0$, $X \to \infty$) resulted in the solutions (51) and (52) for the reflection and transmission coefficients and (54) for the transmitted energy. (Two related problems of interest are considered in the Appendix.) On this basis, it was assumed that when L/λ_0 is small and $X(z)$ is arbitrary, propagation is not dependent upon the details of the electron density distribution but only on the integrated value across the slab. A considerable simplification in the analysis of problems of this type should be obtained therefore from the solution of an equivalent homogeneous slab problem, Eq. (58), with $X = \overline{X}$ = constant defined in (55). The validity of these assertions was examined by comparing the appropriate exact and approximate expressions for a wide range of conditions. The virtually identical results obtained for $L/\lambda_0 \ll 1$ (in particular, $L/\lambda_0 = 0.001$ and 0.01)

established the basic premise regarding the dependence on $\bar{X}$ which, it may be noted, can be used in a wide class of problems apart from the present general boundary value problem outlined in Section II.

Complete agreement became more than acceptable correlation when L/λ_0 was increased to 0.1. Indeed, a maximum discrepancy of seven percent was found in the calculations covering the full range of transmission levels of possible interest corresponding to the conditions, $X_1 = 2.25$, 25, 100, 400; $Z = 0.01$, 1, 10; $Y = 0$, 5, 100. A further correlation at $L/\lambda_0 = 0.5$ was derived in which the degree of accuracy depended on the values of these parameters. This information is of value as a complement to the extensive results given in Section III for $L/\lambda_0 = 0.5$ (and, to a lesser extent, $L/\lambda_0 = 1$) when calculations are required at other values of X_1, Z, Y, or in the transitional region of 0.1 to 1.0.

The problem of a re-entry cone which was previously treated[2] assuming a homogeneous plasma is considered once again in Section III. A, using a triangular distribution of $X(z)$. The geometry and cases are specified in Fig. 3 and the results are shown in Figs. 4a through 4c. The increase in transmission predicted by the more realistic inhomogeneous plasma formulation is quite pronounced. Further, the magnetic field required to provide a specified acceptable level of transmission can be substantially larger assuming a homogeneous plasma. In Fig. 4a, for example (f = 240 Mc, u = 26,000 fps), at 100,000 ft, 1200 gauss, 3600 gauss, and 7800 gauss would be required to obtain 15 db, 10 db, and 5 db, respectively, for a homogeneous plasma. The corresponding values specified by the inhomogeneous plasma calculalations are 0, 1400, and 4200 gauss, a significant decrease of practical interest. The detailed values for this typical re-entry application are shown in the aforementioned graphs. The obvious utility of the results of the small L/λ_0 analysis is clearly demonstrated by its application to the re-entry cone problem. Good agreement was obtained between the exact values shown in Figs. 4a and 4b and the corresponding limiting algebraic expression results [Eq. (54)]. Excellent agreement was obtained in all cases when the more general approximate expression, (58), is used, including the conditions in Fig. 4c at which $|\text{in}_0\bar{n}*L|$ is no longer small.
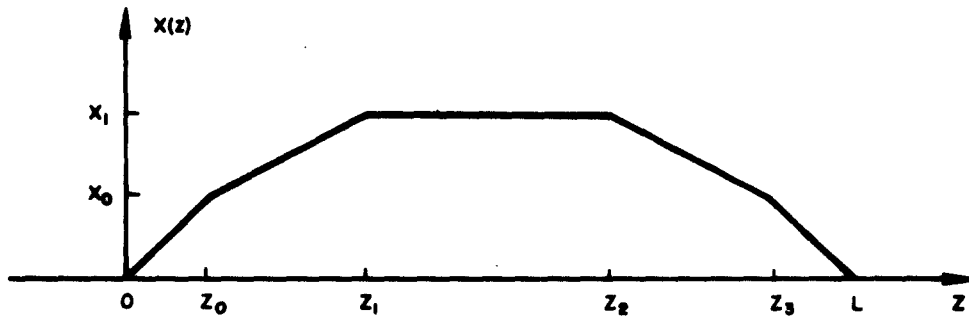
SECTION VI

FIGURES

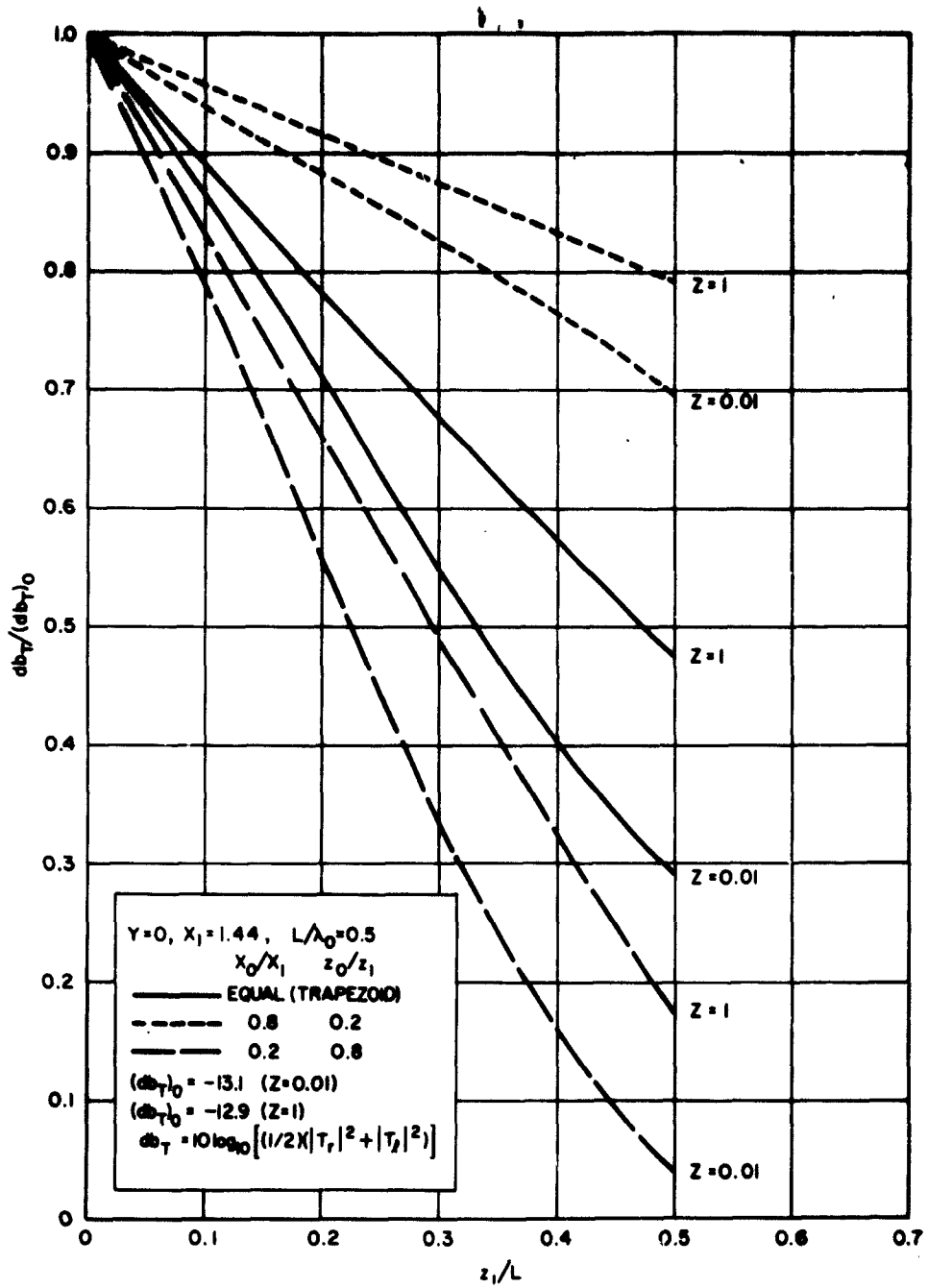Fig. 1. Kinked-trapezoid distribution of X(z); Eq. (12).
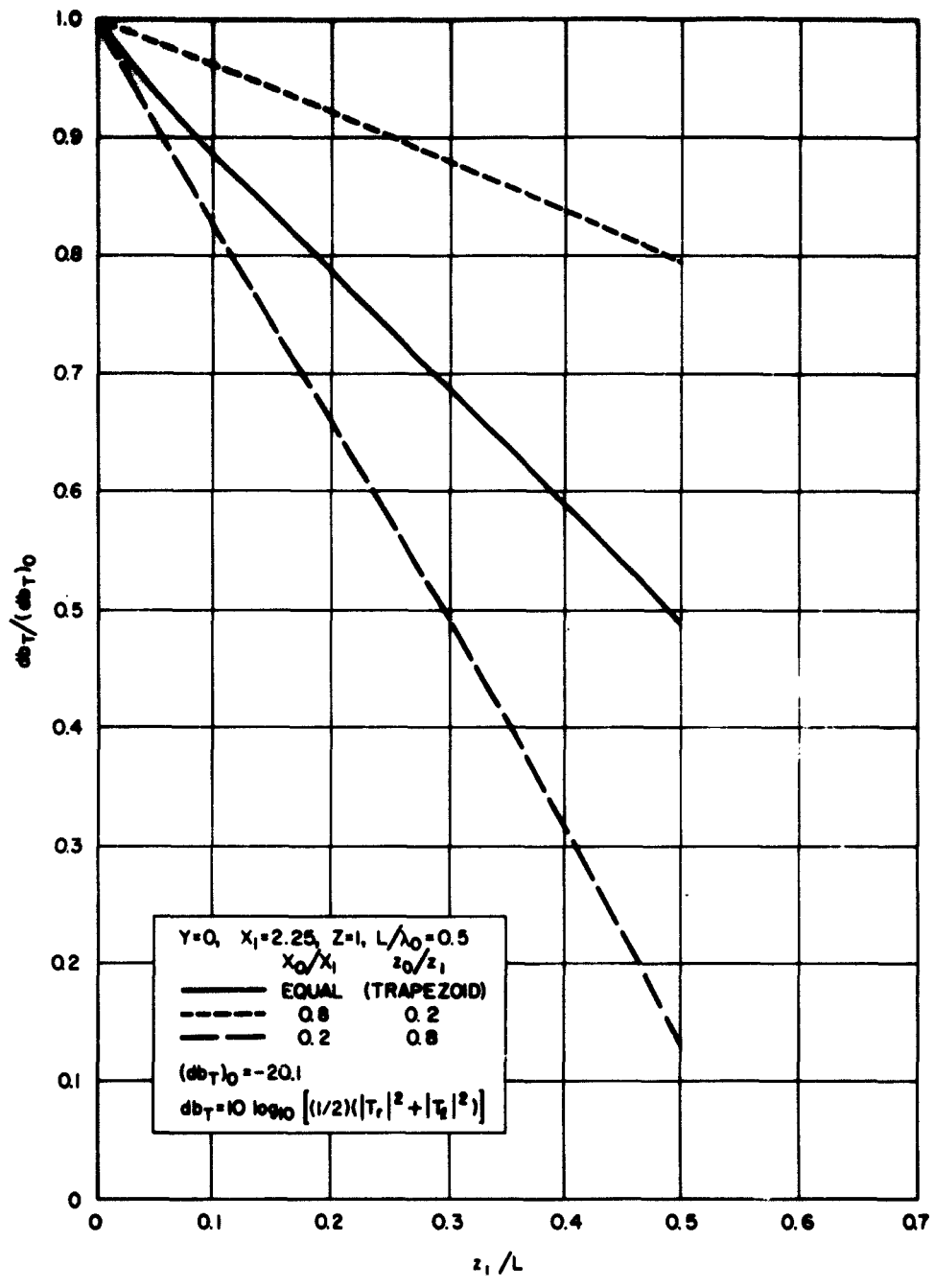
Fig. 2a. Transmitted energy, kinked trapezoid X(z).

Fig. 2b. Transmitted energy, kinked trapezoid X(z) (continued).

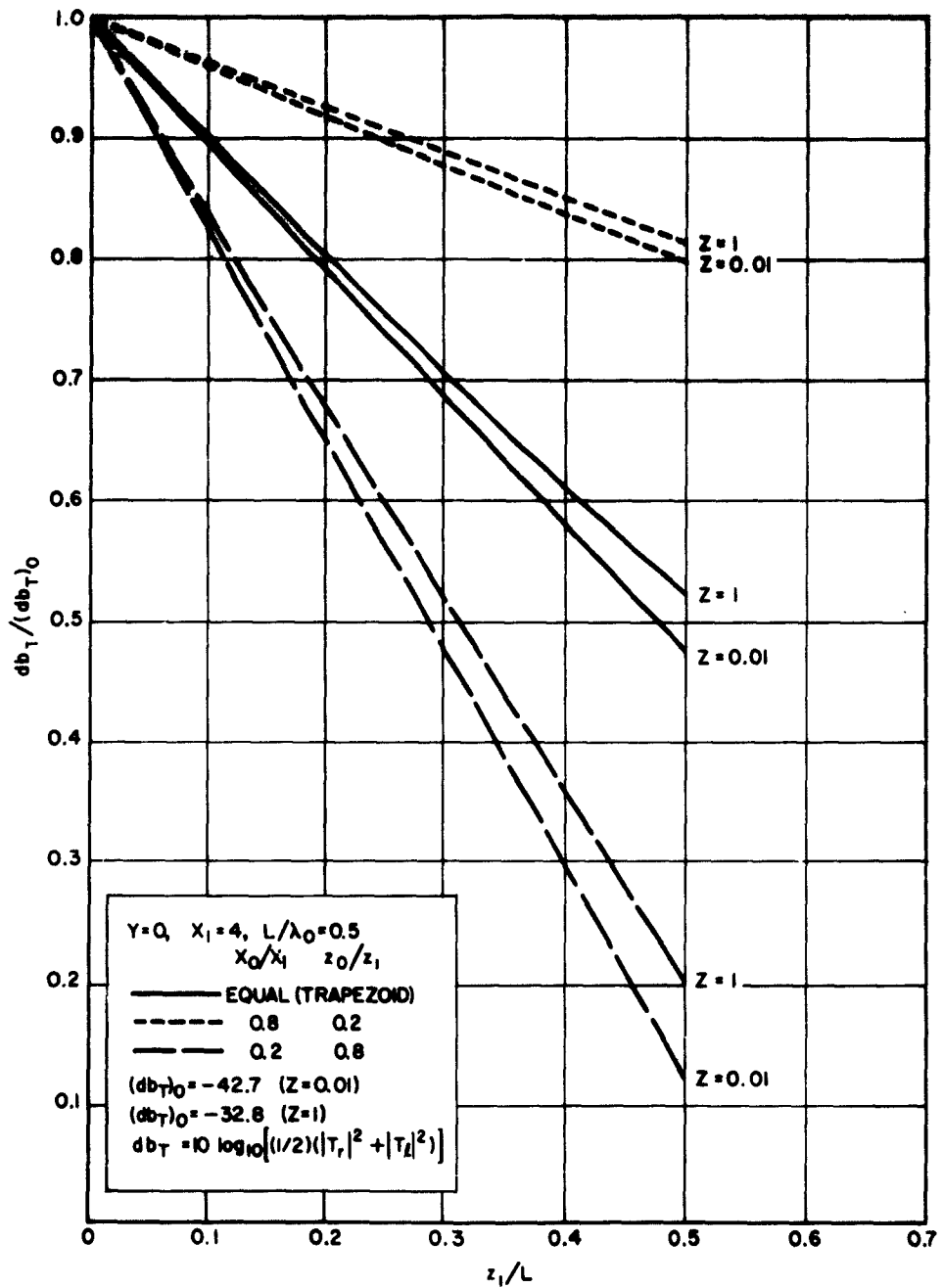$db_T/(db_T)_0$

1.0

0.9

0.8
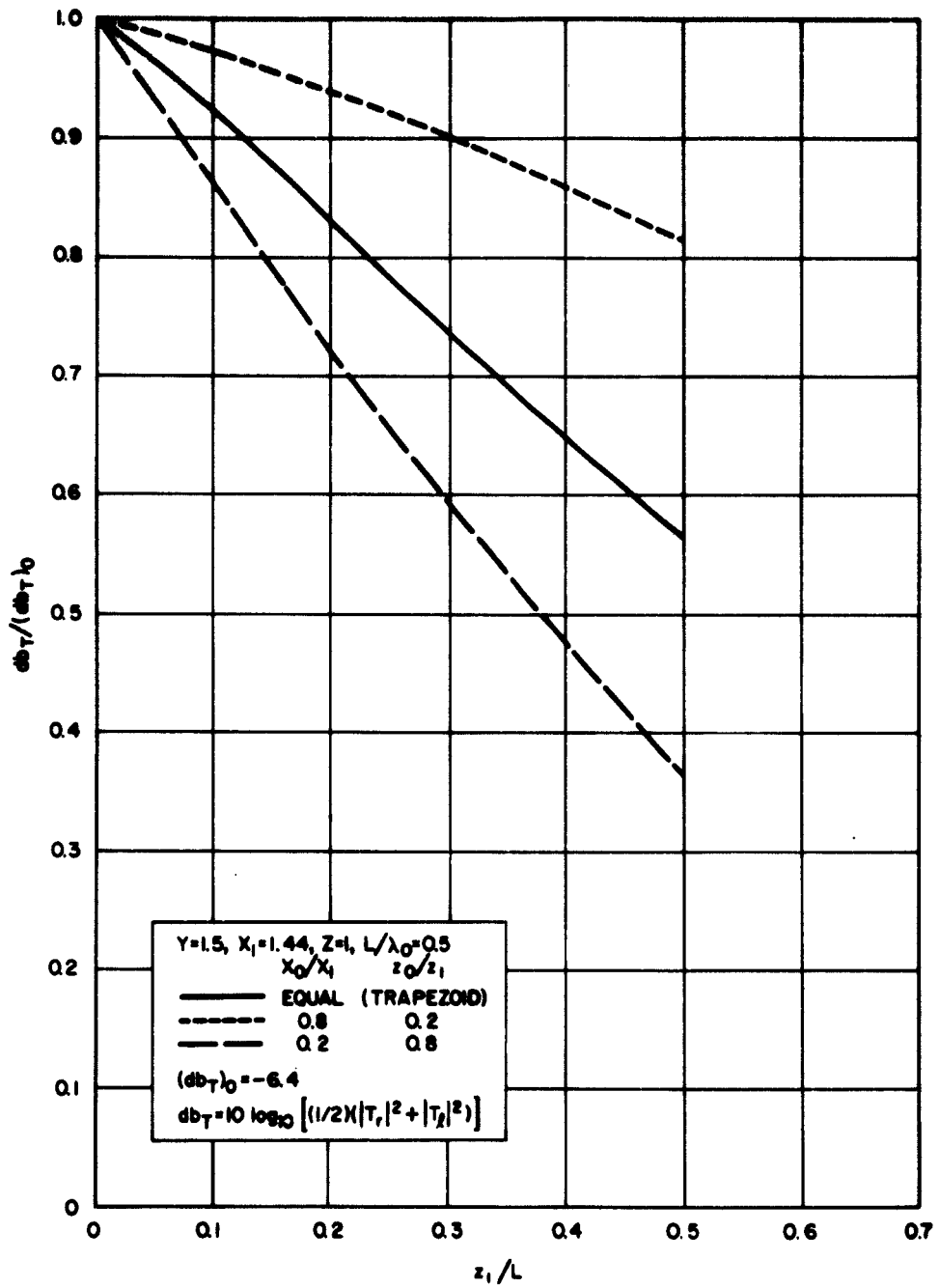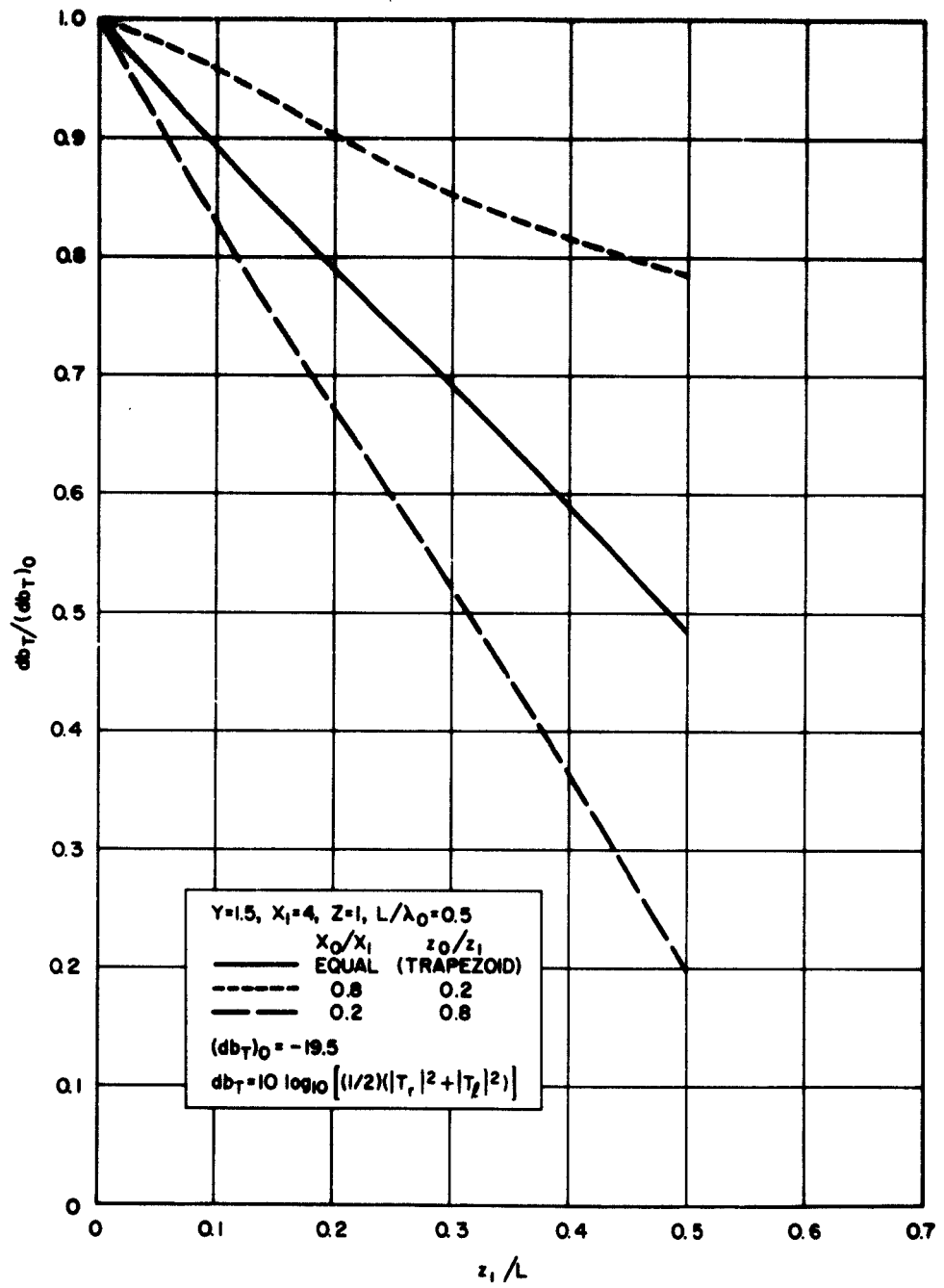
$Z=1$
$Z=0.01$

0.7

0.6

0.5

$Z=1$

$Z=0.01$

0.4

0.3

$Y=0, \quad X_1=4, \quad L/\lambda_0=0.5$

$\quad X_0/X_1 \qquad z_0/z_1$

—————— EQUAL (TRAPEZOID)

- - - - - - 0.8   0.2

— — — 0.2   0.8

$(db_T)_0 = -42.7 \quad (Z=0.01)$

$(db_T)_0 = -32.8 \quad (Z=1)$

$db_T = 10 \log_{10}\left[(1/2)(|T_r|^2 + |T_\ell|^2)\right]$

0.2

$Z=1$

$Z=0.01$

0.1

0   0.1   0.2   0.3   0.4   0.5   0.6   0.7

z_1/L

Fig. 2c. Transmitted energy, kinked trapezoid X(z) (continued).

Fig. 2d.   Transmitted energy, kinked trapezoid X(z) (continued).

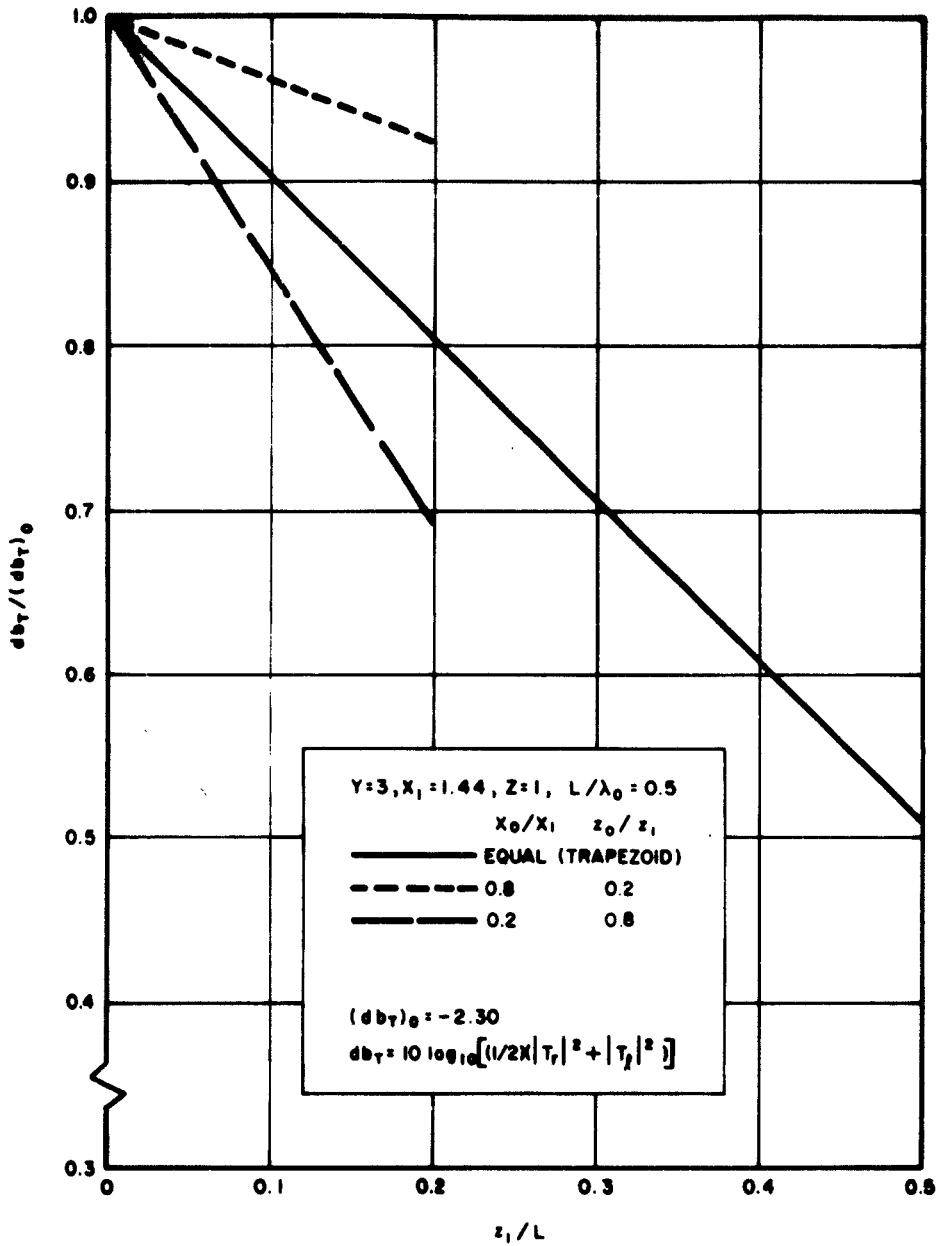Fig. 2e. Transmitted er.ergy, kinked trapezoid X(z) (continued).

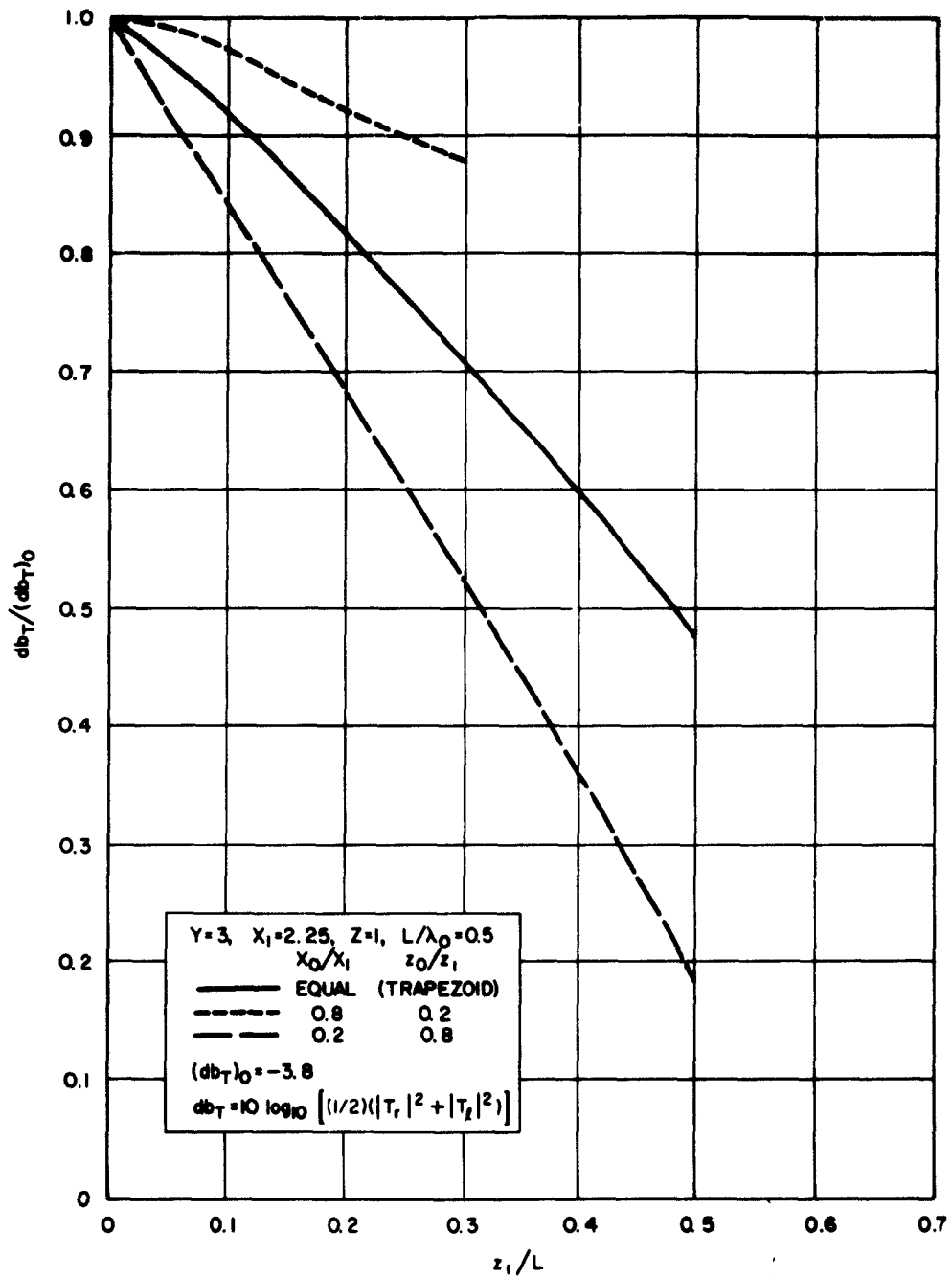Fig. 2f. Transmitted energy, kinked trapezoid X(z) (continued).

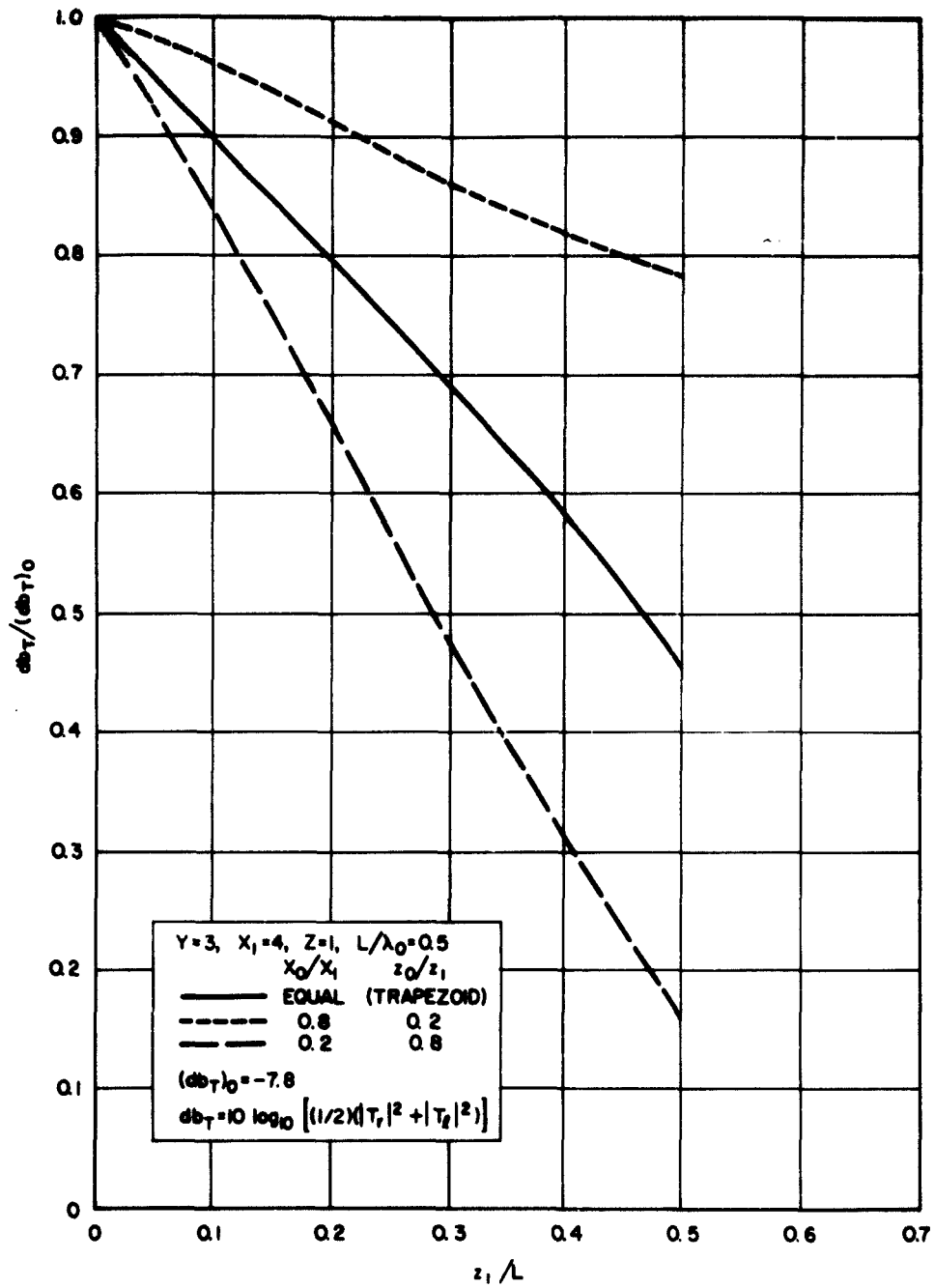Fig. 2g. Transmitted energy, kinked trapezoid $X(z)$ (continued).

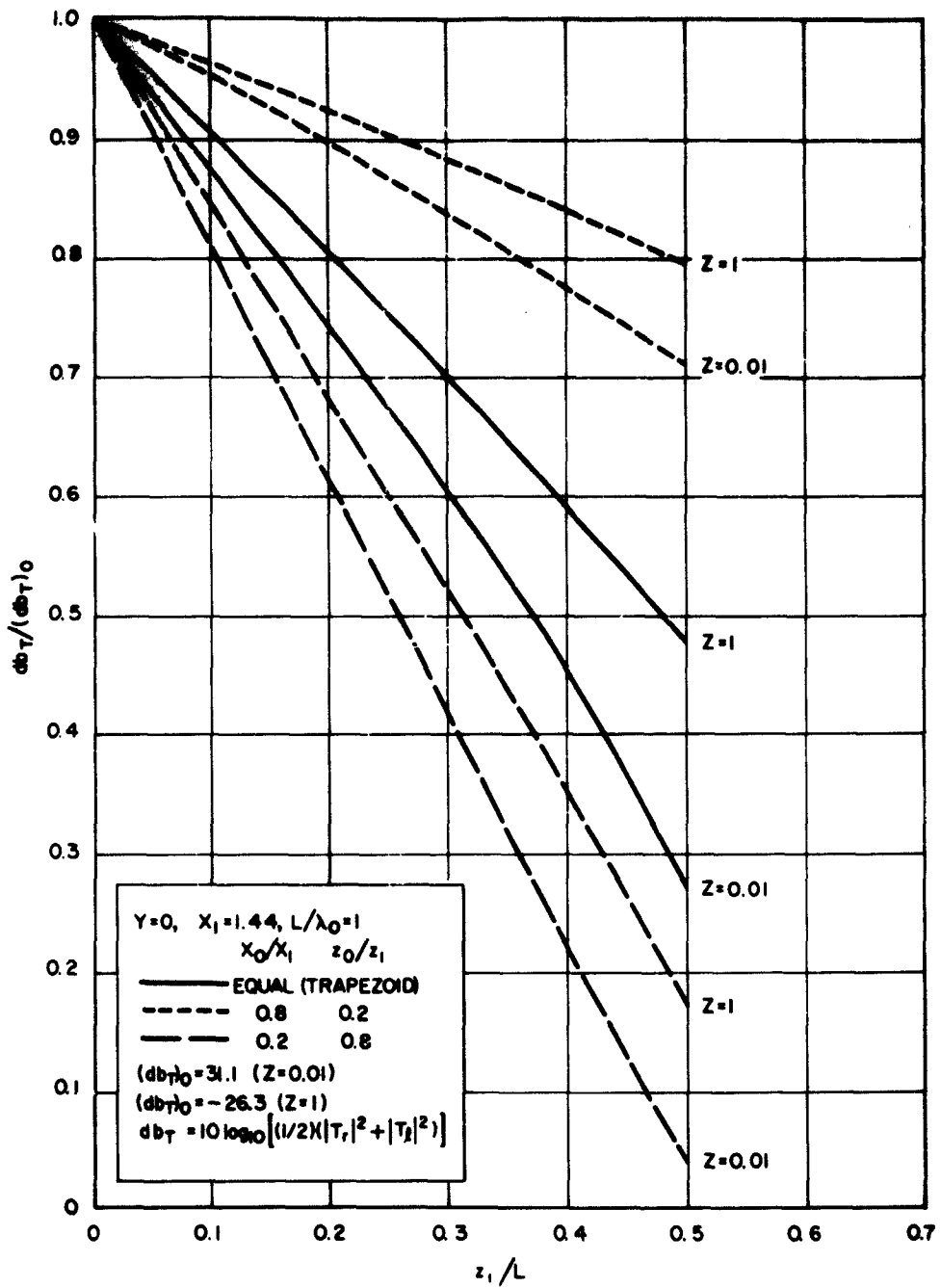Fig. 2h. Transmitted energy, kinked trapezoid X(z) (continued).

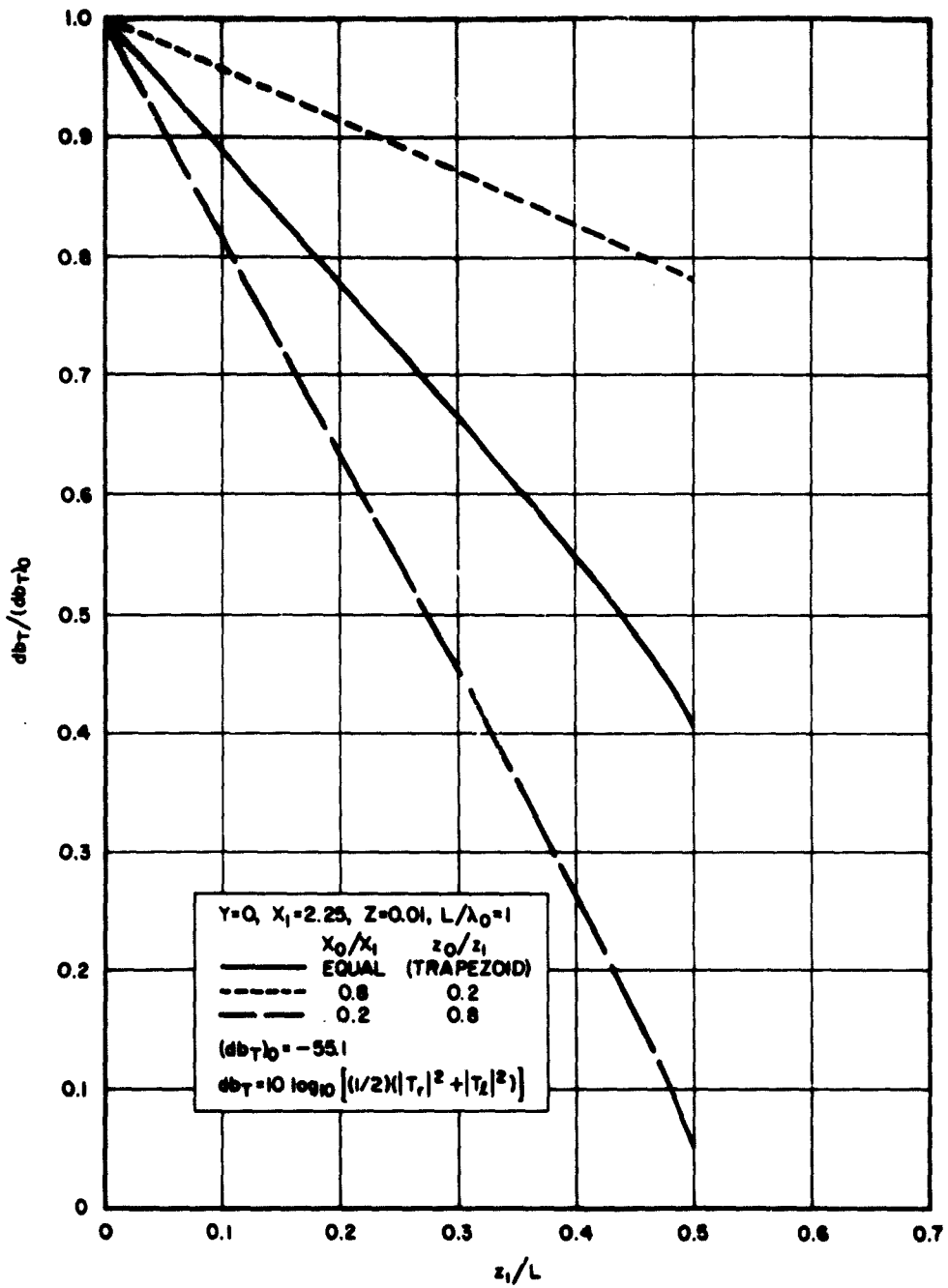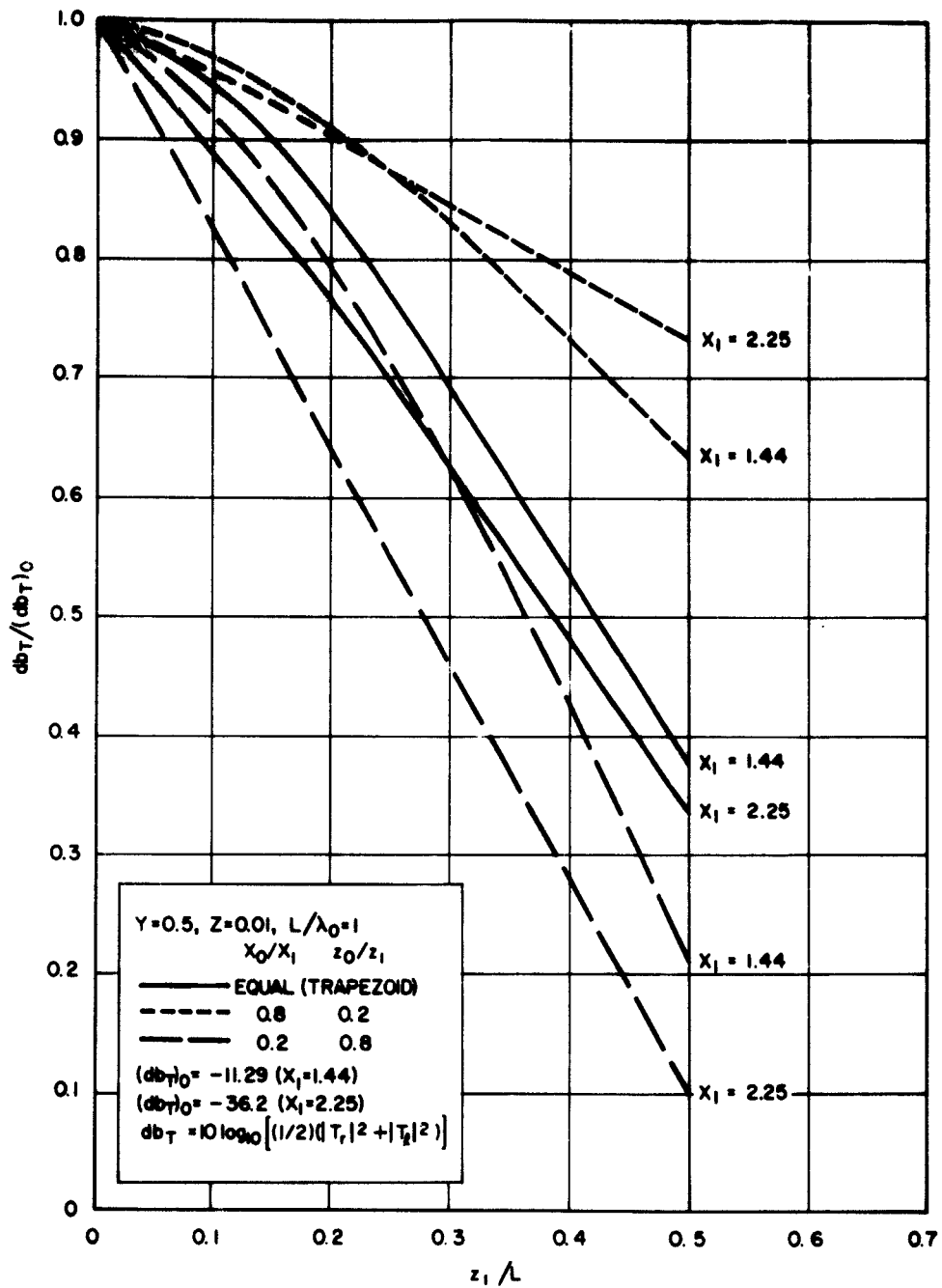Fig. 2i. Transmitted energy, kinked trapezoid X(z) (continued).

-43-

Fig. 2j. Transmitted energy, kinked trapezoid X(z) (continued).

-44-

Fig. 2k. Transmitted energy, kinked trapezoid X(z) (continued).
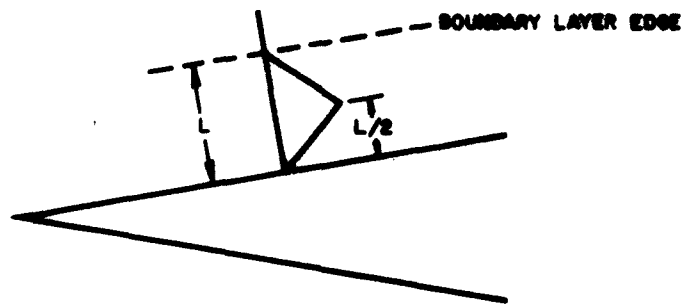
-45-

Fig. 3. Re-entry 10° cone at zero angle of attack. Inhomogeneous plasma profile, flight conditions.

Altitude (ft)	u (fps)	f (cps)	L/λ_0	X_1	Z
50,000	26,000	2.4×10^8	0.000952	47,000	175
		3×10^9	0.0119	301	14
	23,600	2.4×10^8	0.000952	26,400	158
100,000	26,000	2.4×10^8	0.00325	11,700	20.4
		3×10^9	0.0406	74.8	1.63
	23,600	2.4×10^8	0.00325	1,740	17.5
150,000	26,000	2.4×10^8	0.01	1,285	2.38
		3×10^9	0.125	8.22	0.19
	23,600	2.4×10^8	0.01	146	1.96

Fig. 4a. Transmitted energy, re-entry 10° cone at zero angle of attack.

SIGNAL FREQUENCY, $f = 2.4 \times 10^8$ CPS
RE-ENTRY VELOCITY, $u = 23,600$ FPS

———————— HOMOGENEOUS
—— —— —— —— INHOMOGENEOUS

$db_T = 10 \log_{10}\left[(1/2)(|T_r|^2 + |T_l|^2)\right]$

150,000 FT
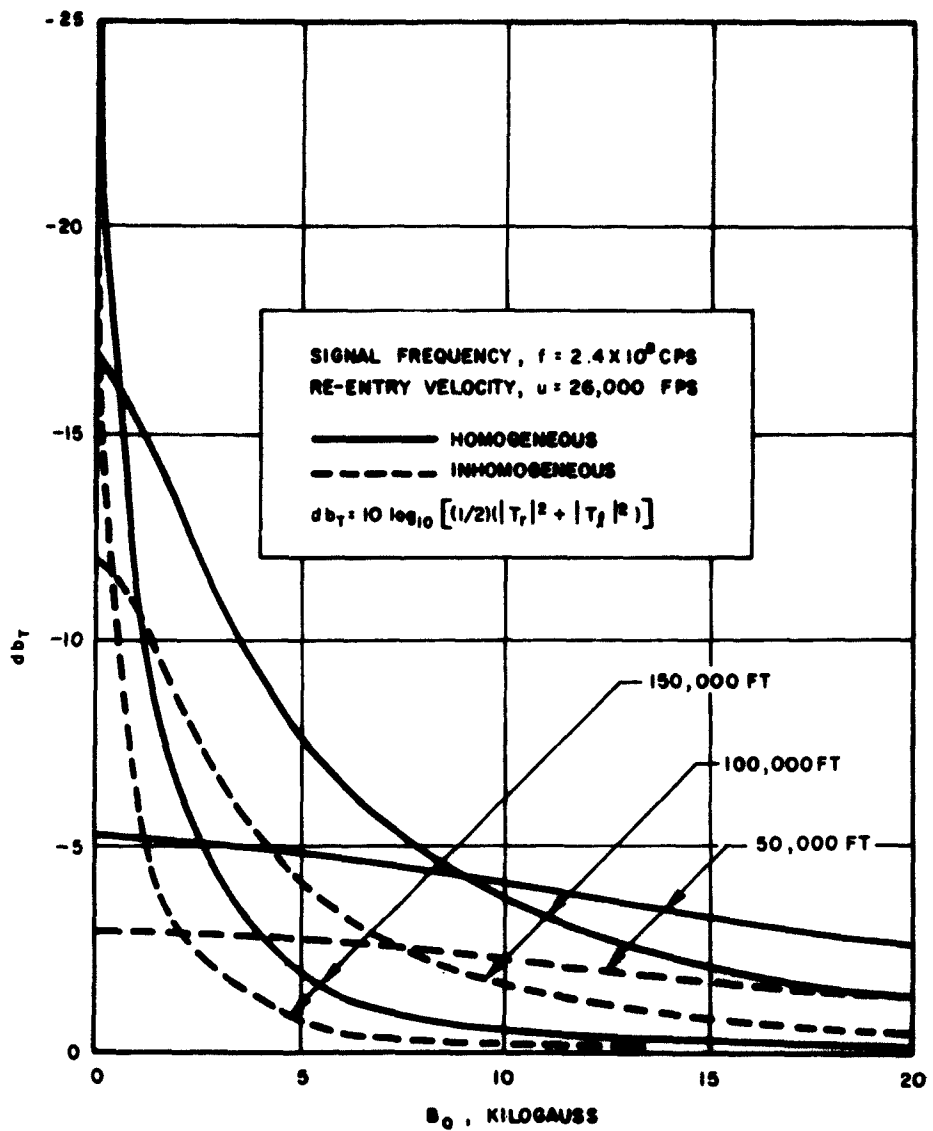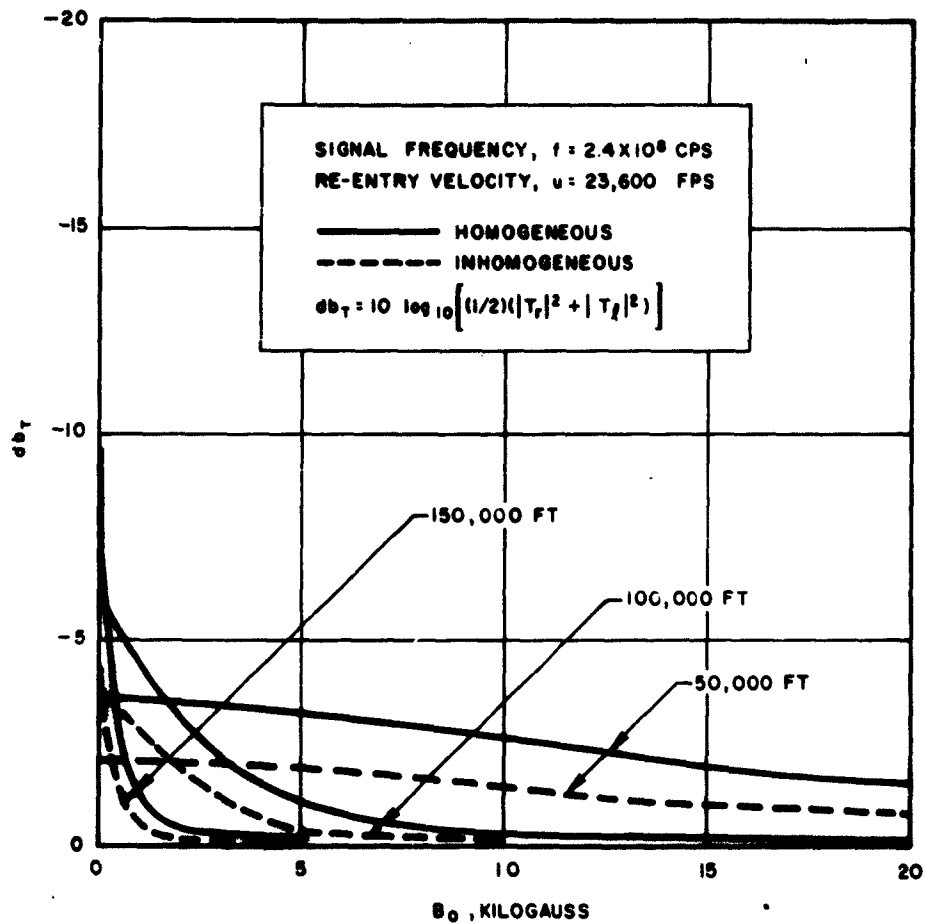
100,000 FT

50,000 FT

B_0 , KILOGAUSS

Fig. 4b. Transmitted energy, re-entry 10° cone at zero angle of attack.
(continued)

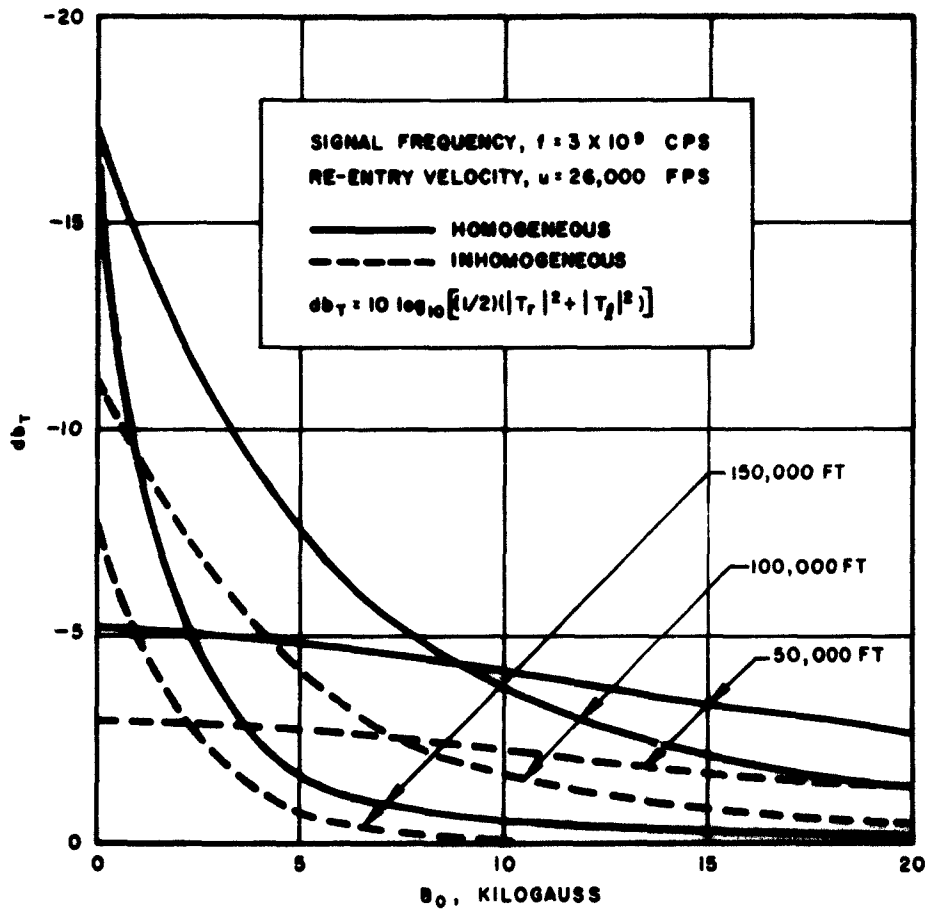Fig. 4c. Transmitted energy, re-entry $10°$ cone at zero angle of attack.
(continued)
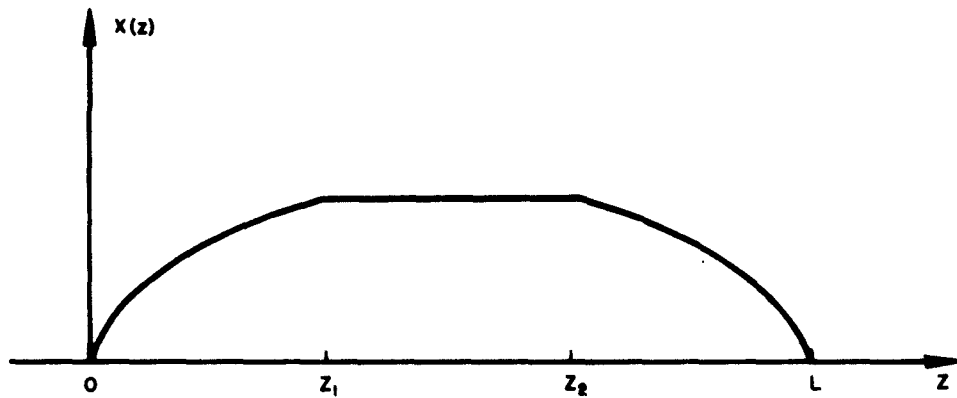
Fig. 5. Exponential-homogeneous-exponential distribution of X(z); Eq. (35).

Fig. 6a. Transmitted energy; exponential X(z).

Fig. 6b. Transmitted energy; exponential X(z) (continued).

-52-

Fig. 6c. Transmitted energy; exponential X(z) (continued).

Fig. 6d.   Transmitted energy; exponential X(z) (continued).

Y = 10, Z = 1, L/λ₀ = 0.5

$Y=10,\ Z=1,\ L/\lambda_0=0.5$

$X_1 = 100 \ ; \ (db_T)_0 = -11.80$

$X_1 = 400 \ ; \ (db_T)_0 = -19.96$

$db_T = 10 \log_{10}\left[(1/2)(|T_r|^2 + |T_\ell|^2)\right]$

$a\lambda_0 = 12$

$a\lambda_0 = 6$

$db_T/(db_T)_0$

z_1/L

Fig. 6e. Transmitted energy; exponential X(z) (continued).

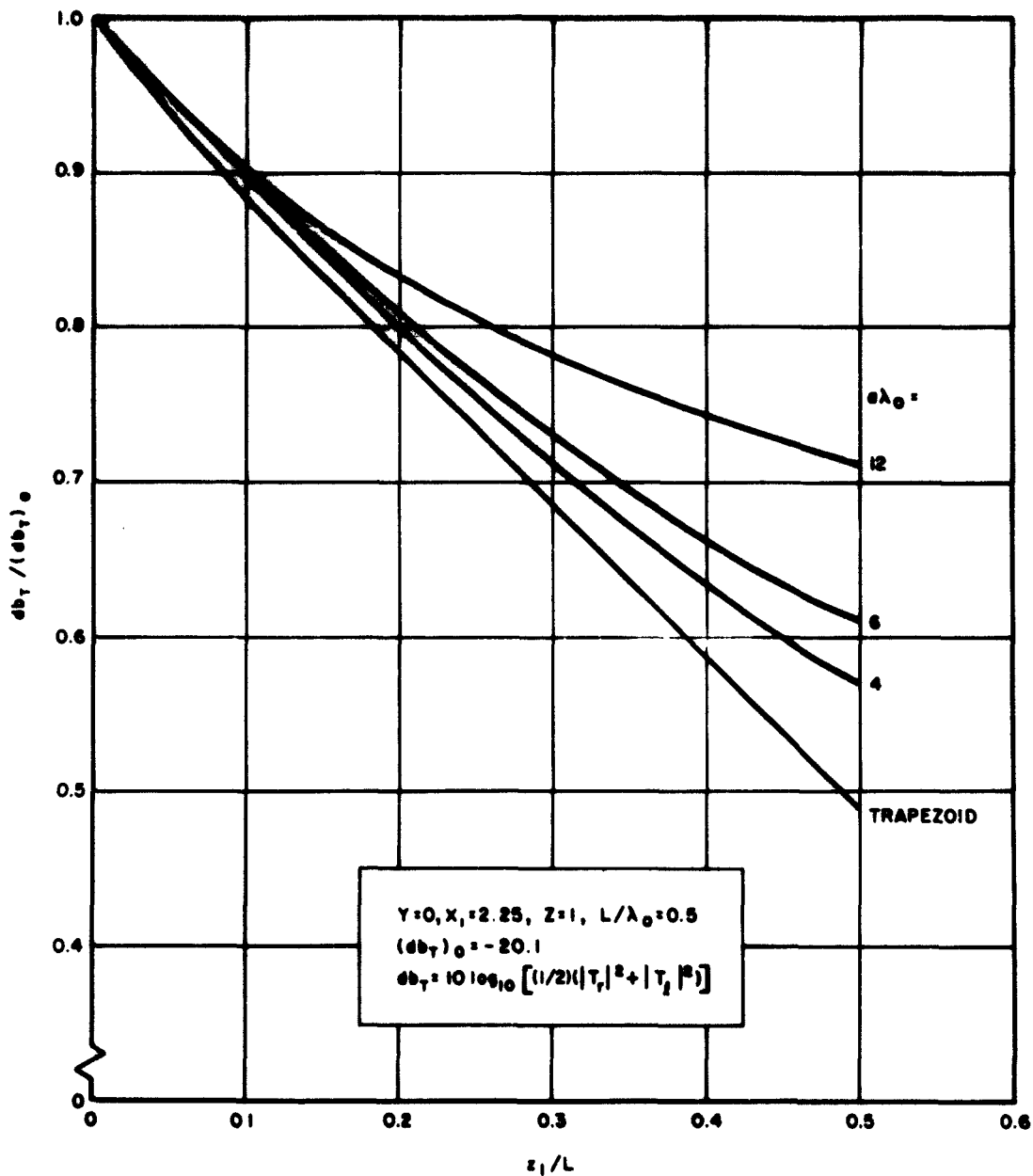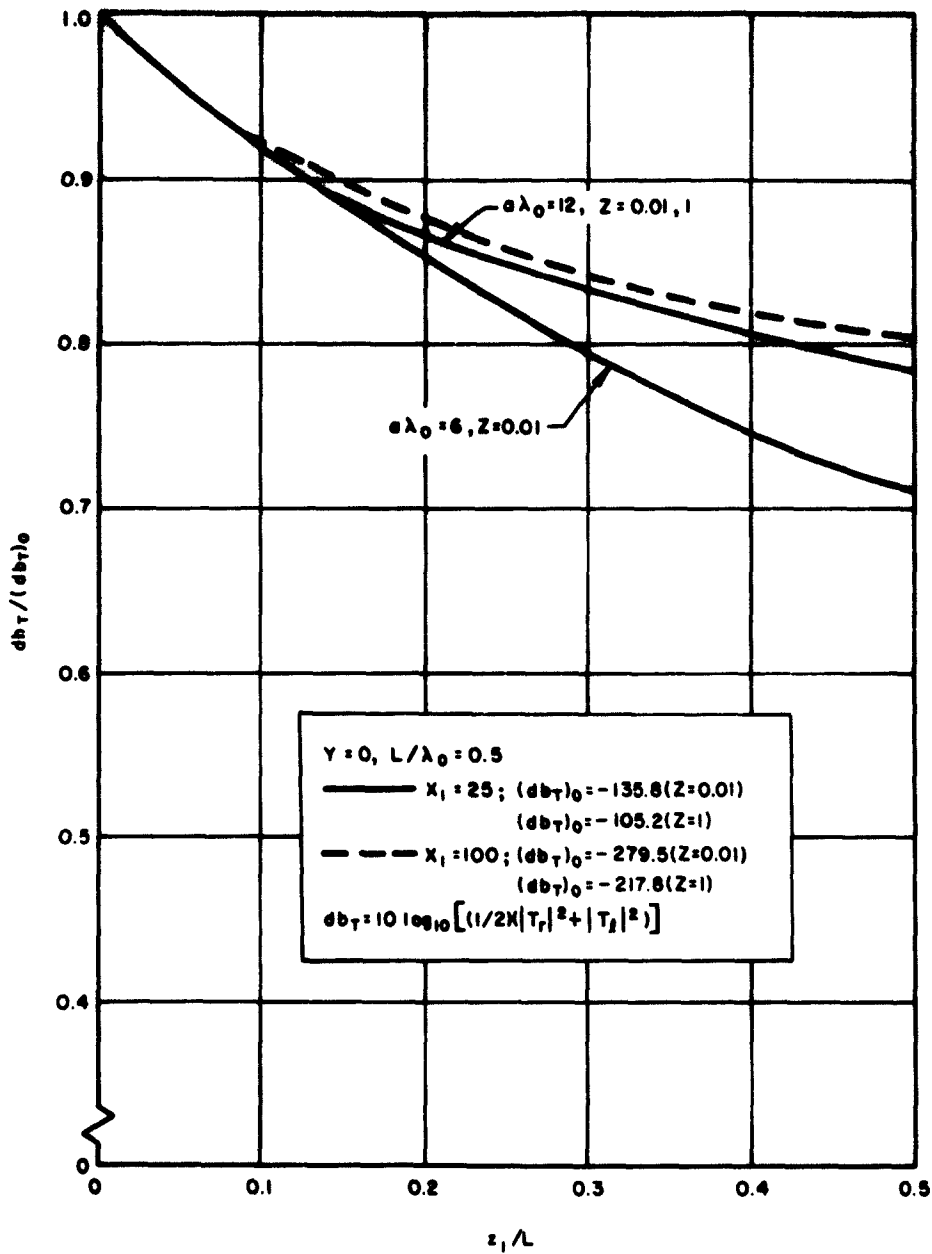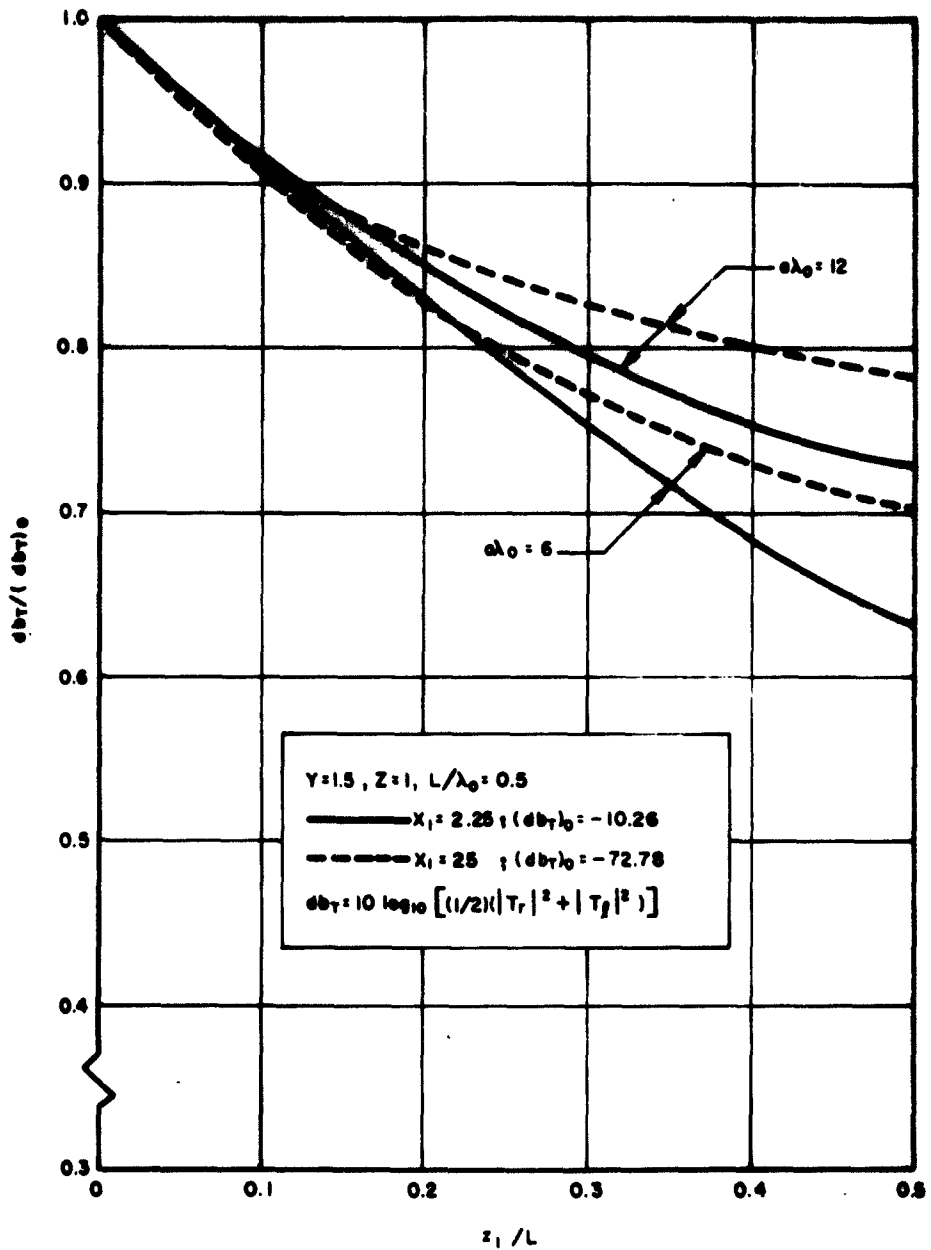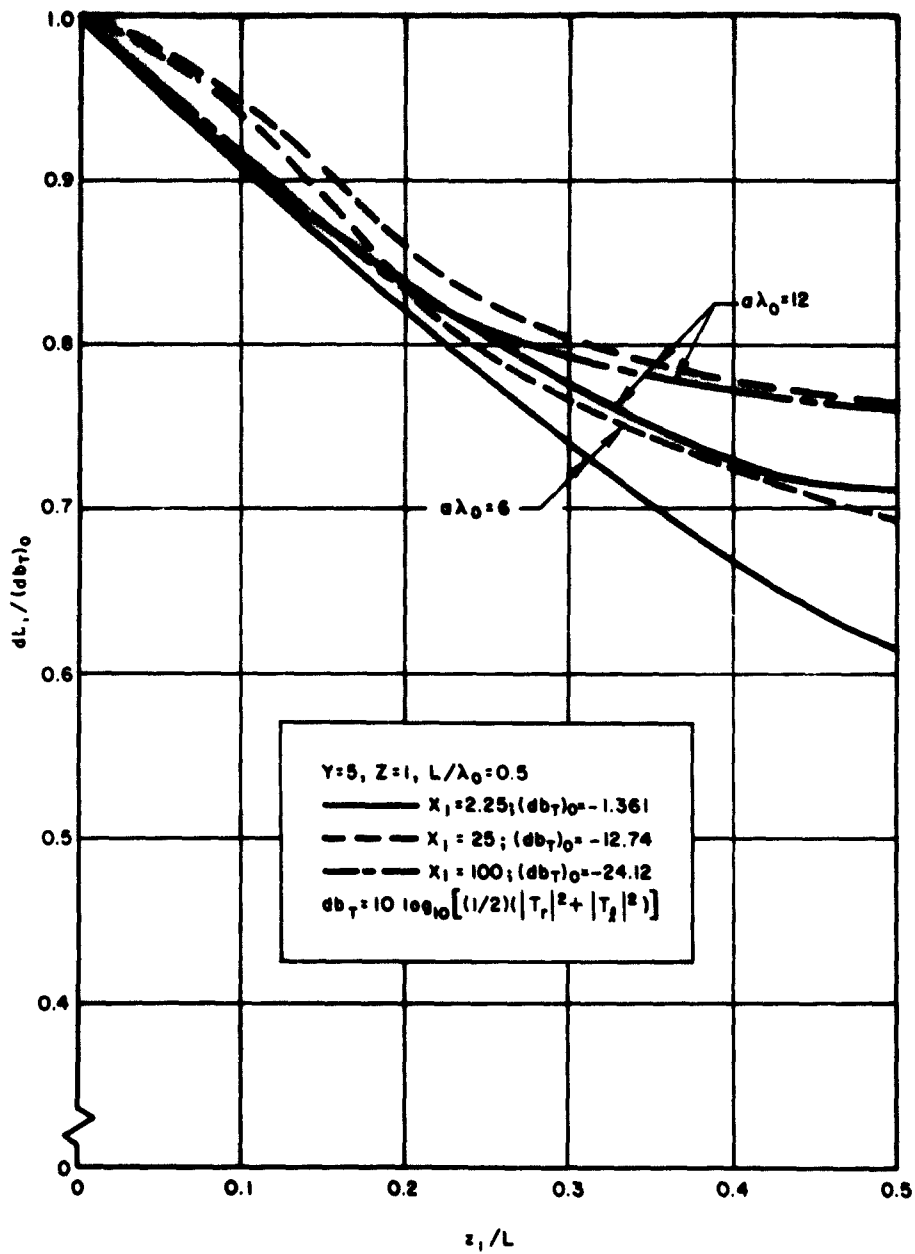Fig. 6f. Transmitted energy; exponential X(z) (continued).

Fig. 6g. Transmitted energy; exponential X(z) (continued).

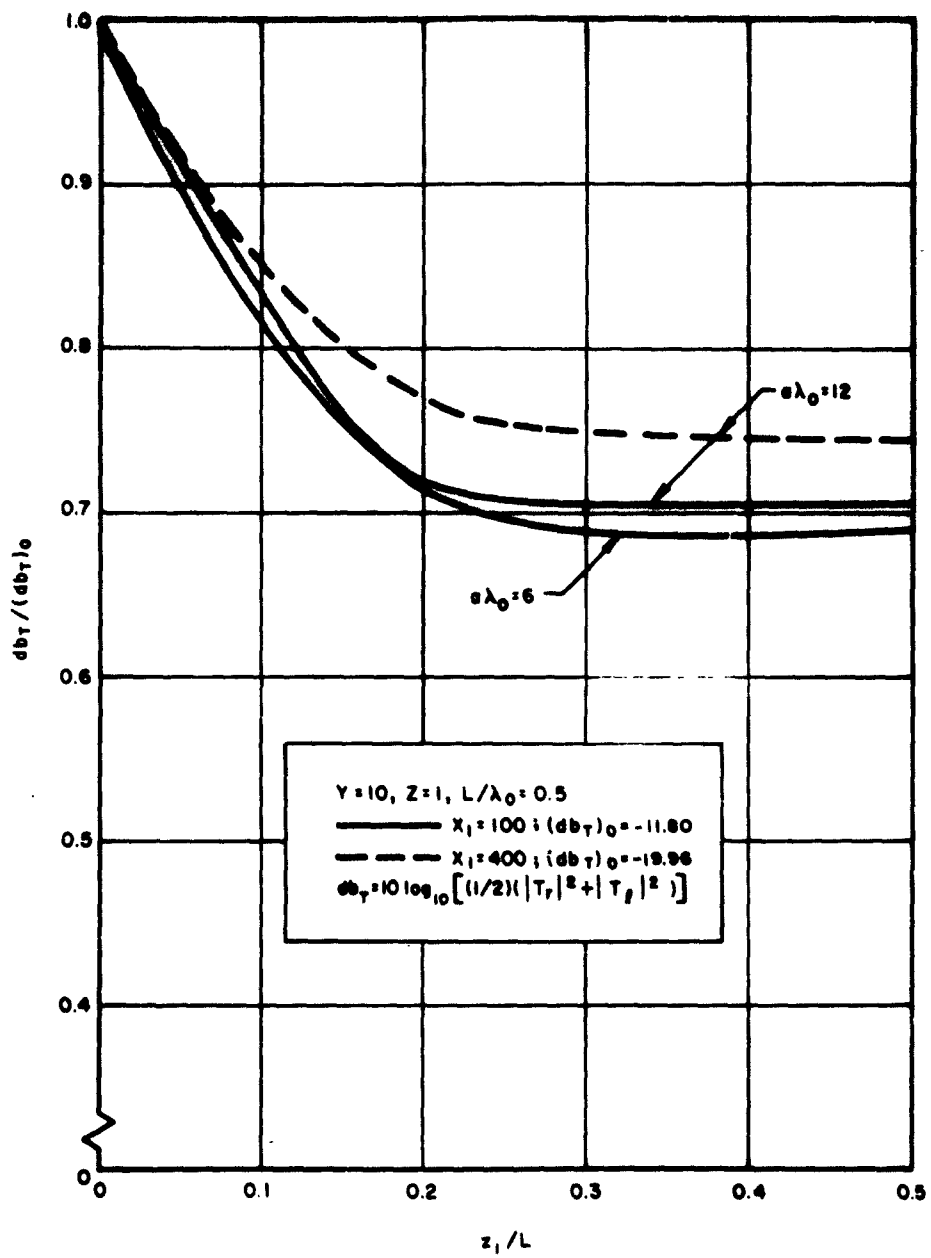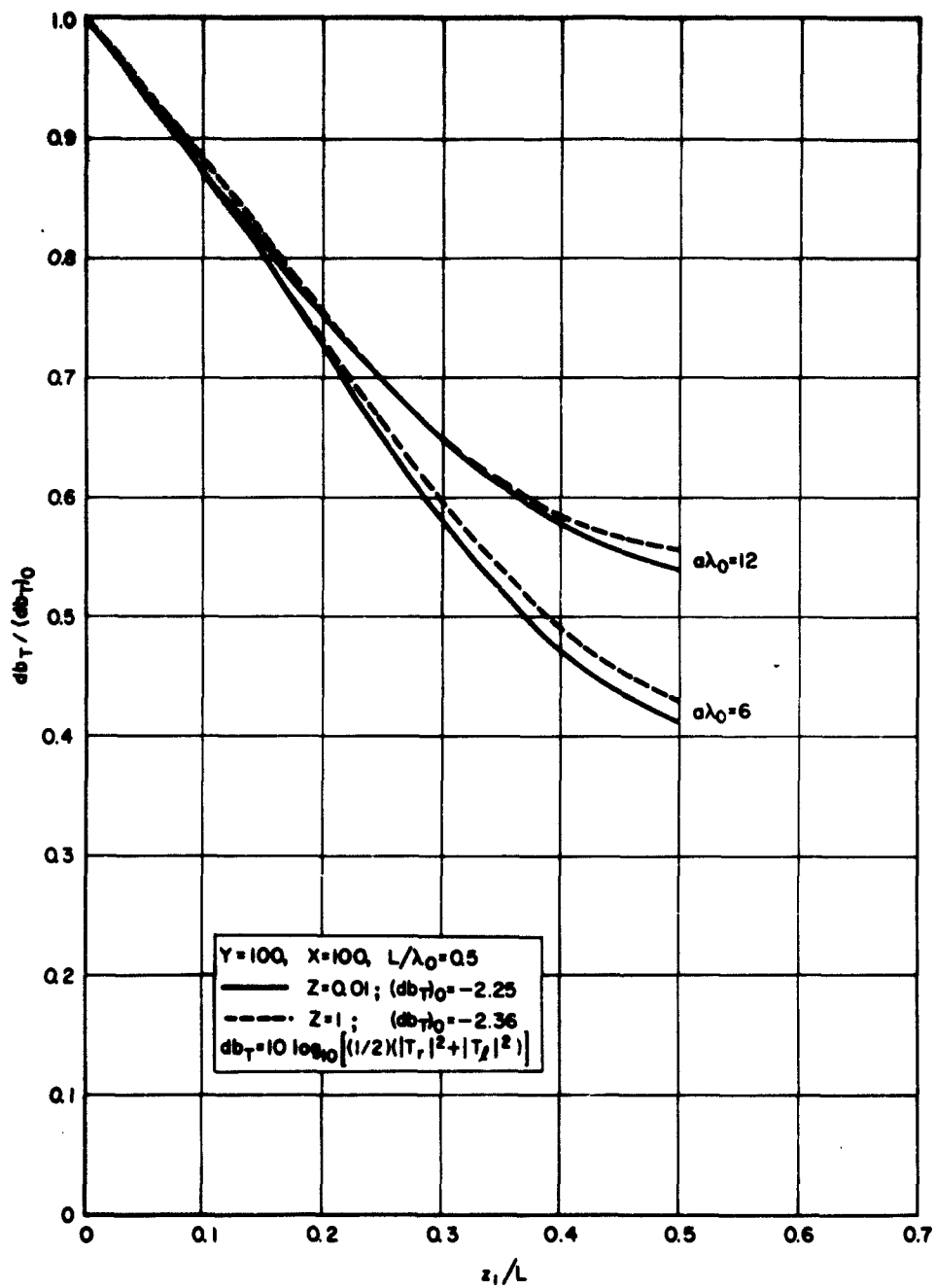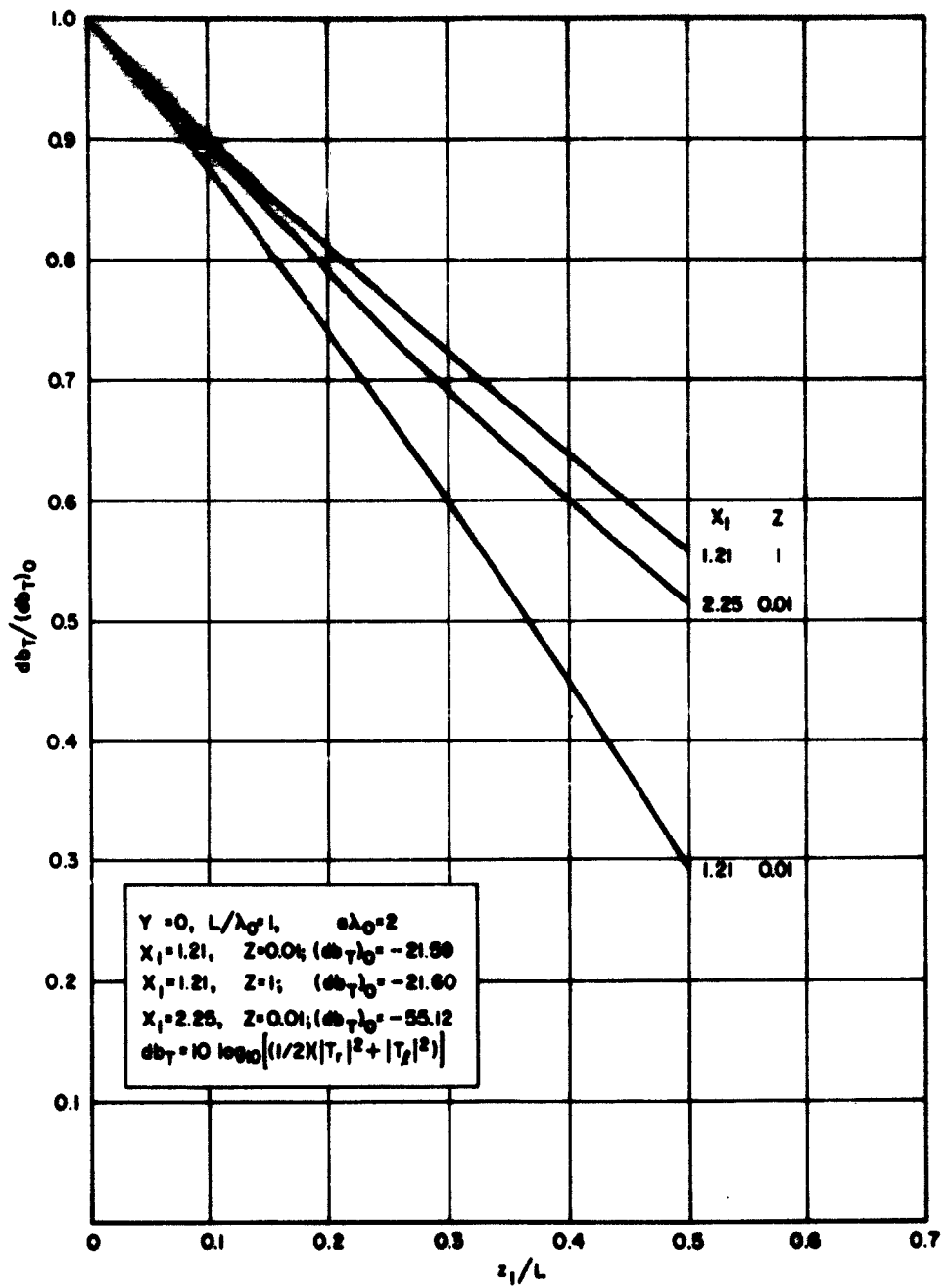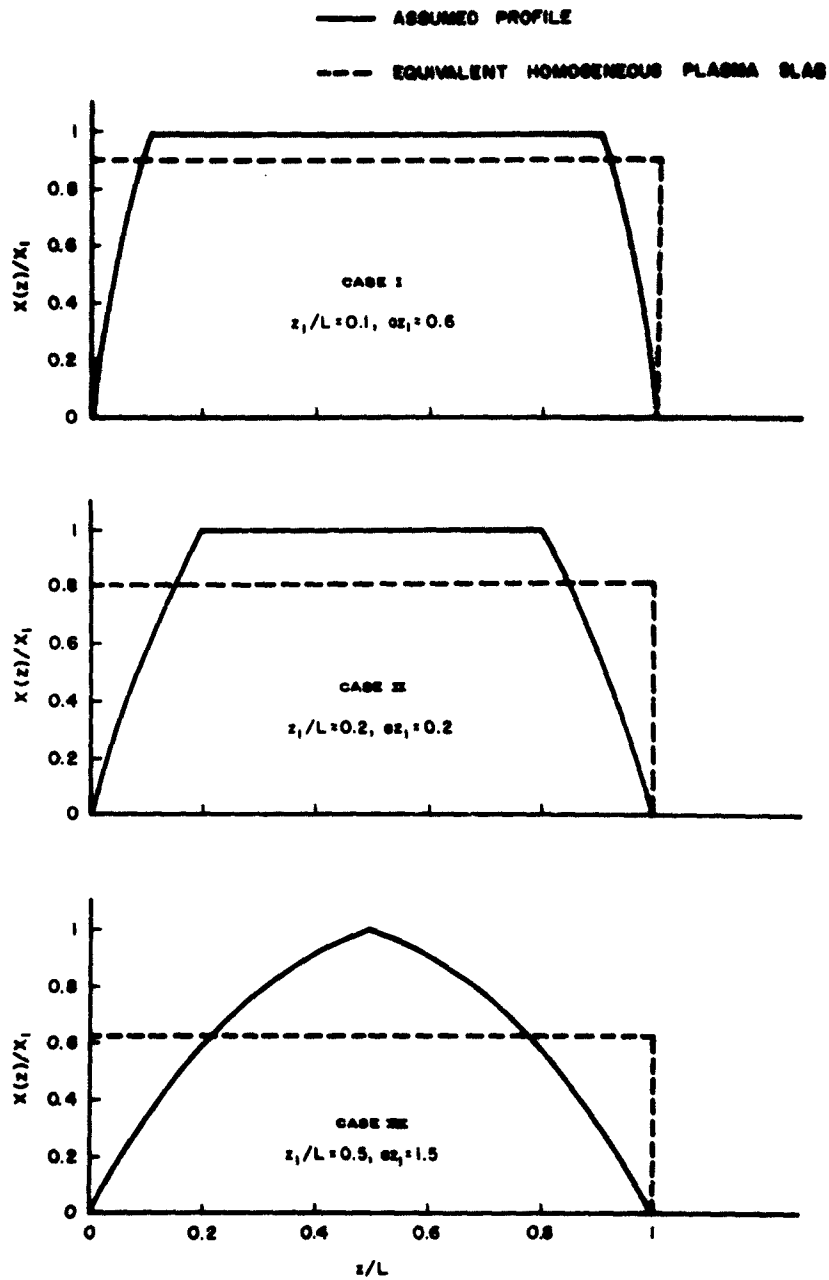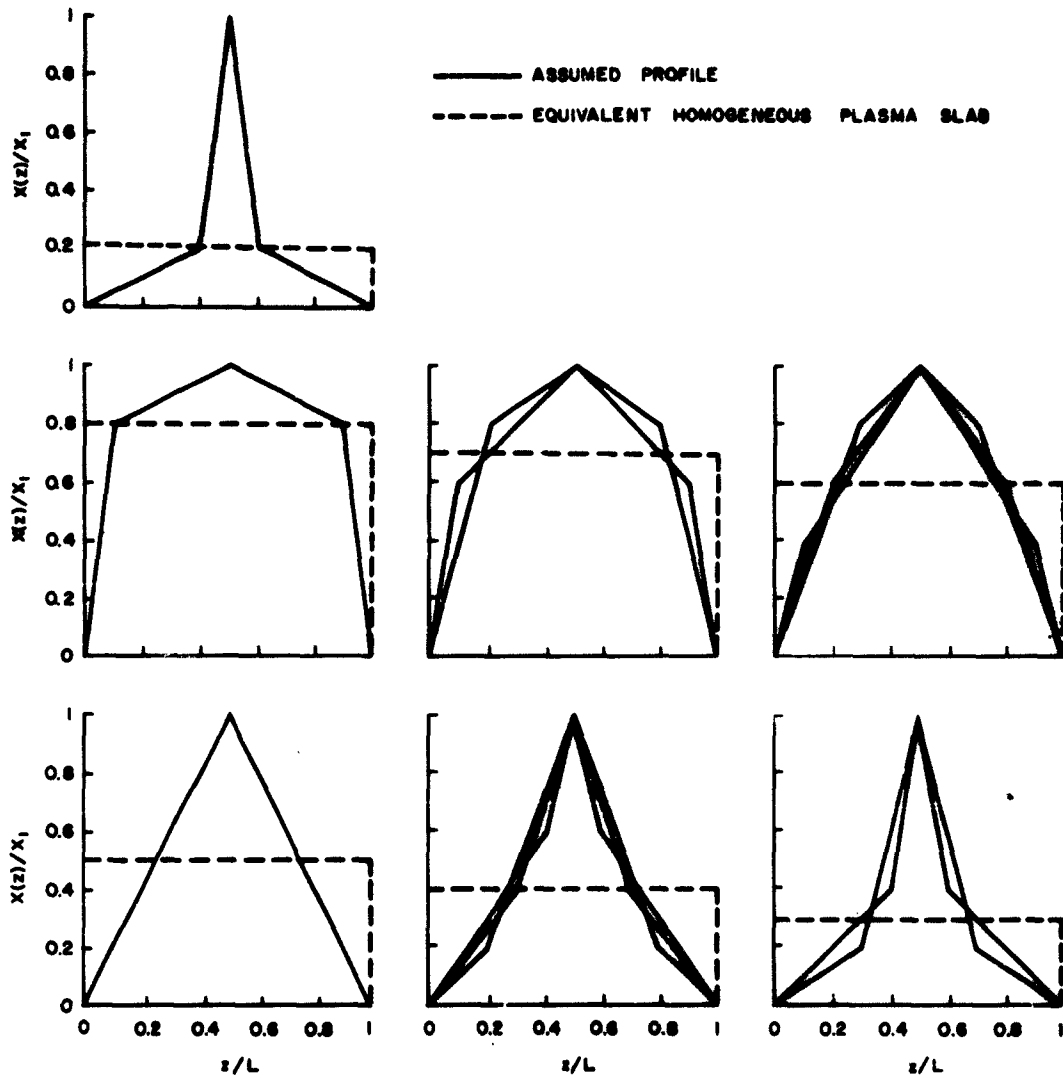Fig. 7. Exponential profiles used for correlation of equivalent homogeneous plasma transmission calculations with exact values.

Fig. 8. Kinked-trapezoid profiles used for correlation of equivalent homogeneous plasma transmission calculations with exact values.

L/λ₀ = 0.5, Y = 0

z	X_0/X_1	x_0/x_1	$\bar{X}/X_1$	$X_1 = 1.44$			$X_1 = 2.25$			$X_1 = 4$		
				db_T exact	db_T homog. $\bar{X}$	$\frac{(db_T)_{exact}}{(db_T)_{\bar{X}}}$	db_T exact	db_T homog. $\bar{X}$	$\frac{(db_T)_{exact}}{(db_T)_{\bar{X}}}$	db_T exact	db_T homog. $\bar{X}$	$\frac{(db_T)_{exact}}{(db_T)_{\bar{X}}}$
1	0.2	0.2	0.5	-6.007	-5.885	1.020	-9.678	-9.767	0.990	-16.93	-17.92	0.945
		0.4	0.4	-4.662	-4.564	1.022	-7.5.5	-7.592	0.991	-13.31	-14.30	0.932
		0.6	0.3	-3.370	-3.305	1.019	-5.439	-5.476	0.992	-9.809	-10.50	0.935
		0.8	0.2	-2.166	-	-	-3.501	-3.458	1.012	-6.455	-6.637	0.973
	0.4	0.2	0.6	-7.366	-7.247	1.018	-11.84	-11.94	0.992	-20.43	-21.30	0.960
		0.6	0.4	-4.674	-4.564	1.025	-7.567	-7.592	0.997	-13.49	-14.30	0.943
		0.8	0.3	-3.401	-3.305	1.028	-5.538	-5.476	1.010	-10.13	-10.50	0.967
	0.6	0.2	0.7	-8.729	-8.655	1.008	-13.94	-14.07	0.993	-23.66	-24.45	0.968
		0.4	0.6	-7.361	-7.247	1.015	-11.79	-11.94	0.986	-20.27	-21.30	0.952
		0.8	0.4	-4.688	-4.564	1.029	-7.614	-7.592	1.003	-13.65	-14.30	0.955
	0.8	0.2	0.8	-10.09	-10.01	1.008	-15.96	-16.14	0.988	-26.65	-27.41	0.973
		0.4	0.7	-8.719	-8.655	1.008	-13.84	-14.07	0.986	-23.35	-24.45	0.954
		0.6	0.6	-7.352	-7.247	1.013	-11.74	-11.94	0.983	-20.12	-21.30	0.944
0.01	0.2	0.2	0.5	-3.712	-1.797	2.065	-9.244	-7.665	1.205	-20.32	-21.37	0.950
		0.4	0.4	-2.500	-0.7474	3.35	-6.366	-4.013	1.59	-15.19	-15.56	0.977
		0.6	0.3	-1.406	-0.2535	5.54	-3.693	-1.407	2.62	-10.04	-8.955	1.121
		0.8	0.2	-0.5542	-	-	-1.502	-0.2928	5.13	-4.998	-2.668	1.87
	0.4	0.2	0.6	-5.166	-3.500	1.473	-12.32	-11.51	1.07	-25.29	-26.46	0.956
		0.6	0.4	-2.343	-0.7474	3.14	-6.212	-4.013	1.55	-15.30	-15.56	0.984
		0.8	0.3	-1.178	-0.2535	4.65	-3.394	-1.407	2.415	-10.15	-8.955	1.133
	0.6	0.2	0.7	-6.987	-5.730	1.22	-15.51	-15.17	1.023	-29.88	-31.02	0.963
		0.4	0.6	-5.333	-3.500	1.523	-12.39	-11.51	1.077	-25.11	-26.46	0.948
		0.8	0.4	-2.226	-0.7474	2.98	-6.128	-4.013	1.55	-15.46	-15.56	0.993
	0.8	0.2	0.8	-9.041	-8.094	1.118	-18.62	-18.56	1.004	-34.08	-35.17	0.970
		0.4	0.7	-7.254	-5.730	1.268	-15.53	-15.17	1.023	-29.48	-31.02	0.951
		0.6	0.6	-5.455	-3.500	1.56	-12.40	-11.51	1.078	-24.91	-26.46	0.941

z	0.01	1	0.01	1	0.01	1
db_T(homog. X_1)	-13.01	-12.80	-24.63	-20.06	-42.54	-32.81

Fig. 9a. Correlation of equivalent homogeneous plasma transmission
calculations with exact values for a kinked-trapezoid profile.

| | | | | L/λ₀ = 0.5, Y = 0.5 | | | | | | | | |
| | | | | X₁ = 1.44 | | | X₁ = 2.25 | | | X₁ = 4 | | |
z	X_0/X_1	s_0/s_1	$\bar{X}/X_1$	db_T exact	db_T homog. $\bar{X}$	$\frac{(db_T)\text{exact}}{(db_T)\bar{X}}$	db_T exact	db_T homog. $\bar{X}$	$\frac{(db_T)\text{exact}}{(db_T)\bar{X}}$	db_T exact	db_T homog. $\bar{X}$	$\frac{(db_T)\text{exact}}{(db_T)\bar{X}}$
1	0.2	0.2	0.5	-5.607	-5.471	1.025	-8.765	-8.633	1.015	-15.239	-15.650	0.9737
		0.4	0.4	-4.461	-4.374	1.020	-6.936	-6.861	1.011	-12.076	-12.466	0.9695
		0.6	0.3	-3.305	-3.281	1.007	-5.141	-5.136	1.001	-8.966	-9.230	0.9736
		0.8	0.2	-2.197	-	-	-3.525	-3.418	1.031	-6.035	-6.087	0.9915
	0.4	0.2	0.6	-6.743	-6.582	1.024	-10.574	-10.437	1.013	-18.327	-18.729	0.9785
		0.6	0.4	-4.462	-4.374	1.020	-6.966	-6.861	1.015	-12.190	-12.456	0.9786
		0.8	0.3	-3.337	-3.281	1.017	-5.214	-5.136	1.015	-9.208	-9.230	0.9976
	0.6	0.2	0.7	-7.868	-7.724	1.019	-12.357	-12.254	1.008	-21.241	-21.660	0.9807
		0.4	0.6	-6.747	-6.582	1.025	-10.562	-10.437	1.012	-18.225	-18.729	0.9731
		0.8	0.4	-4.260	-4.374	0.9739	-6.994	-6.861	1.019	-12.290	-12.456	0.9867
	0.8	0.2	0.8	-8.986	-8.831	1.018	-14.112	-14.063	1.003	-23.904	-24.431	0.9817
		0.4	0.7	-7.881	-7.724	1.020	-12.330	-12.254	1.006	-21.038	-21.660	0.9713
		0.6	0.6	-6.747	-6.582	1.025	-10.544	-10.437	1.010	-18.228	-18.729	0.9733
0.01	0.2	0.2	0.5	-4.069	-3.127	1.301	-7.001	-5.034	1.391	-15.093	-14.194	1.063
		0.4	0.4	-3.411	-2.536	1.345	-5.582	-3.775	1.479	-11.510	-9.626	1.092
		0.6	0.3	-2.470	-1.500	1.647	-4.147	-2.972	1.395	-8.044	-5.605	1.435
		0.8	0.2	-1.271	-	-	-2.563	-1.654	1.550	-4.917	-3.396	1.446
	0.4	0.2	0.6	-4.633	-3.629	1.277	-8.623	-6.955	1.240	-18.762	-18.536	1.012
		0.6	0.4	-3.325	-2.536	1.311	-5.429	-3.775	1.438	-11.409	-9.626	1.185
		0.8	0.3	-2.335	-1.500	1.557	-3.946	-2.972	1.328	-7.869	-5.605	1.393
	0.6	0.2	0.7	-5.321	-4.307	1.235	-10.592	-9.344	1.134	-22.488	-22.500	0.9995
		0.4	0.6	-4.752	-3.629	1.309	-8.788	-6.955	1.264	-18.765	-18.536	1.012
		0.8	0.4	-3.263	-2.536	1.287	-5.317	-3.775	1.408	-11.380	-9.626	1.182
	0.8	0.2	0.8	-6.200	-5.216	1.189	-12.770	-11.912	1.072	-25.832	-26.119	0.9890
		0.4	0.7	-5.572	-4.307	1.294	-10.847	-9.344	1.300	-22.292	-22.500	0.9908
		0.6	0.6	-4.853	-3.629	1.337	-8.904	-6.955	1.280	-18.719	-18.536	1.010

z	0.01	1	0.01	1	0.01	1
db_T(homog. X_1)	-11.163	-7.873	-17.592	-16.951	-29.535	-32.544

Fig. 9b. Correlation of equivalent homogeneous plasma transmission calculations with exact values for a kinked-trapezoid profile (continued).

				L/λ₀ = 0.5, Y = 1.5								
				$X_1 = 1.44$			$X_1 = 2.25$			$X_1 = 4$		
z	X_0/X_1	s_0/s_1	$\bar{X}/X_1$	db_T exact	db_T homog. $\bar{X}$	$\frac{(db_T)_{exact}}{(db_T)_{\bar{X}}}$	db_T exact	db_T homog. $\bar{X}$	$\frac{(db_T)_{exact}}{(db_T)_{\bar{X}}}$	db_T exact	db_T homog. $\bar{X}$	$\frac{(db_T)_{exact}}{(db_T)_{\bar{X}}}$
1	0.2	0.2	0.5	-3.4892	-3.4534	1.01367	-5.2447	-5.0362	1.0414	-9.3517	-8.9757	1.0419
		0.4	0.4	-2.8575	-2.8574	1.00003	-4.2504	-4.1533	1.0234	-7.3874	-7.0597	1.0464
		0.6	0.3	-2.2170	-2.2695	0.97687	-3.2661	-3.2799	0.9958	-5.5160	-5.3387	1.0332
		0.8	0.2	-1.5752	-	-	-2.2988	-2.3478	0.9791	-3.7934	-3.7654	1.0074
	0.4	0.2	0.6	-4.0948	-4.0143	1.02005	-6.2288	-5.9619	1.0448	-11.3537	-11.0430	1.0281
		0.6	0.4	-2.8634	-2.8777	0.9950	-4.2539	-4.1533	1.0242	-7.4017	-7.0597	1.0484
		0.8	0.3	-2.2323	-2.2695	0.9836	-3.2864	-3.2799	1.0020	-5.5627	-5.2798	1.0536
	0.6	0.2	0.7	-4.6852	-4.5816	1.0226	-7.2285	-6.9465	1.0406	-13.3790	-13.1776	1.01528
		0.4	0.6	-4.1016	-4.0143	1.0217	-6.2489	-5.9619	1.0481	-11.3543	-11.0430	1.0282
		0.8	0.4	-2.8693	-2.8777	0.9971	-4.2574	-4.1533	1.0251	-7.4208	-7.0597	1.0511
	0.8	0.2	0.8	-5.2666	-5.1371	1.0252	-8.2623	-7.9942	1.0335	-15.3940	-15.3121	1.00
		0.4	0.7	-4.7070	-4.5817	1.0273	-7.2769	-6.9465	1.0476	-9.3363	-13.1776	0.7085
		0.6	0.6	-4.1050	-4.0143	1.0226	-6.2617	-5.9619	1.0503	-11.3389	-11.0430	1.0268
0.01	0.2	0.2	0.5	-0.3175	-0.5123	0.6196	-0.9119	-0.5468	1.6677	-2.1353	-2.1939	0.9733
		0.4	0.4	-0.2770	-0.4039	0.6860	-0.5257	-0.5715	0.9199	-1.8191	-0.8171	2.2263
		0.6	0.3	-0.4015	-0.2581	1.5556	-0.5183	-0.4852	1.0682	-0.9686	-0.5320	1.8207
		0.8	0.2	-0.3105	-	-	-0.4624	-0.2770	1.6693	-0.6910	-0.5497	1.2570
	0.	0.2	0.6	-0.5345	-0.5665	0.9435	-1.1193	-0.5379	2.0870	-3.1903	-3.9567	0.8063
		0.6	0.4	-0.2388	-0.4039	0.5912	-0.4934	-0.5715	0.8633	-1.6021	-0.8171	1.9607
		0.8	0.3	-0.2232	-0.2581	0.8648	-0.3119	-0.4852	0.6428	-0.8788	-0.5320	1.6519
	0	0.2	0.7	-0.7438	-0.5685	1.3084	-1.2182	-0.7681	1.5860	-4.9404	-5.1985	0.9504
		0.4	0.6	-0.5794	-0.5665	1.0228	-1.2960	-0.5379	2.4094	-2.9328	-3.9567	0.7412
		0.8	0.4	-0.2082	-0.4039	0.5155	-0.4988	-0.5715	0.8728	-1.5695	-0.8171	1.9208
	0.8	0.2	0.8	-0.7588	-0.5414	1.4016	-1.1964	-1.3870	0.8626	-8.2681	-5.3745	1.5384
		0.4	0.7	-0.8916	-0.5685	1.5683	-1.5739	-0.7681	2.0491	-4.3914	-5.1985	0.8447
		0.6	0.6	-0.5794	-0.5665	1.0228	-1.3924	-0.5379	2.5886	-2.7452	-3.9567	0.6938

Fig. 9c. Correlation of equivalent homogeneous plasma transmission calculations with exact values for a kinked-trapezoid profile (continued).

z	x_0/X_1	s_0/s_1	$\bar{X}/X_1$	db_T exact	db_T homog. $\bar{X}$	$\frac{(db_T)_{exact}}{(db_T)\bar{X}}$	db_T exact	db_T homog. $\bar{X}$	$\frac{(db_T)_{exact}}{(db_T)\bar{X}}$	db_T exact	db_T homog. $\bar{X}$	$\frac{(db_T)_{exact}}{(db_T)\bar{X}}$
					$X_1 = 1.44$			$X_1 = 2.25$			$X_1 = 4$	
1	0.2	0.2	0.5	-1.174	-1.166	1.009	-1.836	-1.795	1.032	-3.461	-3.289	1.051
		0.4	0.4	-0.9620	-0.9426	1.020	-1.495	-1.444	1.034	-2.733	-2.571	1.062
		0.6	0.3							-2.056	-1.914	1.073
		0.8	0.2							-1.367	-1.489	1.060
	0.4	0.2	0.6							-4.265	-4.005	1.042
		0.6	0.4	-0.9950	-0.9426	1.012	-1.482	-1.444	1.027	-2.710	-2.571	1.053
		0.8	0.3							-1.997	-1.914	1.043
	0.6	0.2	0.7							-5.141	-4.955	1.038
		0.4	0.6							-4.290	-4.085	1.050
		0.8	0.4	-0.9491	-0.9426	1.007	-1.471	-1.444	1.019	-2.692	-2.571	1.048
	0.8	0.2	0.8							-	-	-
		0.4	0.7							-5.191	-4.955	1.048
		0.6	0.6							-4.297	-4.085	1.051
0.01	0.2	0.2	0.5	-0.0917	-0.0274	3.35		< -0.2		-0.6778	-0.4388	1.545
		0.4	0.4							-0.6063	-0.2328	2.60
		0.6	0.3							-0.5222	-0.1046	5.00
		0.8	0.2							-0.2798	-0.0362	7.73
	0.4	0.2	0.6	< -0.1						-0.9513	-0.7443	1.28
		0.6	0.4							-0.5252	-0.2328	2.255
		0.8	0.3							-0.3367	-0.1046	3.22
	0.6	0.2	0.7							-1.430	-1.159	1.234
		0.4	0.6							-0.9991	-0.7443	1.342
		0.8	0.4							-0.4542	-0.2328	1.952
	0.8	0.2	0.8							-	-	-
		0.4	0.7							-	-1.159	-
		0.6	0.6							-1.021	-0.7443	1.572

z	0.01	1	0.01	1	0.01	1
db_T(homog. X_1)	-0.1732	-2.302	-0.6168	-3.778	-2.537	-7.742

*Numbers are not given below when the magnitude of db_T is too small to be of practical interest.

Fig. 9d. Correlation of equivalent homogeneous plasma transmission calculations with exact values for a kinked-trapezoid profile (continued).

APPENDIX

We shall consider first the propagation of a horizontally polarized wave which is obliquely incident on a vanishingly thin isotropic plasma sheath. The governing equation for the electric field intensity is now given by[2]

$$E_y'' + n_0^2 \left(C^2 - \frac{X}{U} \right) E_y = 0 \quad , \quad C = \cos \theta_I \quad , \tag{A-1}$$

where θ_I is the angle of incidence, i.e., the angle formed by the wave normal of the incident wave and the positive z-axis. A similar procedure to the one employed at the outset of Section IV leads quite readily to the following results:

$$R = \frac{-\overline{X} n_0 L/U}{2iC + \overline{X} n_0 L/U} \quad , \tag{A-2}$$

$$T = \frac{1}{1 - (in_0 L/2C)\overline{X}/U} \quad , \tag{A-3}$$

$$\epsilon_T = |T|^2 = \frac{1 + Z^2}{1 + [Z + (\pi/C)(L/\lambda_0)\overline{X}]^2} \quad . \tag{A-4}$$

These expressions reduce to the corresponding ones for the case of normal incidence ($\theta_I = 0$) derived in Section IV.

The function $\epsilon_T(\theta_I)$ is a maximum at $\theta_I = 0$, decreasing monotonically to zero at $\theta_I = \pm 90$ degrees. Since ϵ_T depends only on $\overline{X}$, we are led again to the assumption of an equivalent homogeneous plasma slab, in which case,

$$T = \frac{(4/C)(\overline{n}*^2 - S^2)^{1/2} \exp(in_0 CL)}{[1 + (\overline{n}*^2 - S^2)^{1/2}/C]^2 \exp\left[in_0 L(\overline{n}*^2 - S^2)^{1/2}\right] - [1 - (\overline{n}*^2 - S^2)^{1/2}/C] \exp\left[-in_0 L(\overline{n}*^2 - S^2)^{1/2}\right]} \tag{A-5}$$

-64-

where $S = \sin \theta_I$ and $\bar{n}*^2 = (1 - X/U)$. This expression will reduce to (A-3) in the present problem when the magnitude of $in_0\bar{n}*L$ is small. The extensive correlation made in Section IV for $\theta_I = 0$ between the values obtained from the approximate expression (58) [or (52), if applicable] and the appropriate exact results can now be used to justify the use of (A-5) [or (A-3)] in the following way: For given X, Z, and L/λ_0 ($Y = 0$), Eq. (A-3) is the same as (52) if we consider a new value of L/λ_0 which is modified by the factor $1/C$. It might be anticipated that the excellent agreement obtained in this correlation for $L/\lambda_0 \leq 0.1$ and the subsequent discussion for $L/\lambda_0 = 0.5$ are an indication of the accuracy afforded by (A-5) in the present problem for the corresponding conditions

$$\frac{L}{\lambda_0} \leq 0.1 \cos \theta_I \quad , \quad \frac{L}{\lambda_0} = 0.5 \cos \theta_I \quad . \tag{A-6}$$

The preceding extension to the case of oblique incidence ($Y = 0$) is certainly tentative in many respects. It is felt, however, that (A-3) or (A-5) can be used to give approximate results in many applications, with qualitative limitations provided by the correlation of Section IV along with the modification (A-6). As a final footnote, we shall consider the following even more tentative, but possibly useful, reasoning when $Z = Z(z)$. In general

$$w'' + n_0^2(C^2 - mX)w = 0 \quad , \tag{A-7}$$

where $w = F$ and $C = 1$ (normal incidence) when there is an applied magnetic field; $w = E_y$ for $Y = 0$; and $m = (U \mp Y)^{-1}$ is now a function of z. The previous limiting calculations can be altered accordingly and we obtain

$$R = \frac{-In_0}{2iC + In_0} \quad , \tag{A-8}$$

$$T = \frac{1}{1 - (in_0 I)/2C} \quad , \tag{A-9}$$

where

$$I = \int_0^L m(z)X(z)dz \quad . \tag{A-10}$$

It seems reasonable to suggest that these limiting results may be used to make approximate calculations including a variable $Z(z)$ when $L/\lambda_0 \ll 1$ and $\left| in_0 L(mX)_{max} \right|$ is less than one.

REFERENCES

1.   R. Mason and R. R. Gold. "Electromagnetic Wave Propagation Through Inhomogeneous Plasmas in the Presence of Applied Magnetic Fields." Presented at the Third Symposium on the Engineering Aspects of Magnetohydrodynamics, Univerity of Rochester, 28-29 March 1962.

2.   R. Mason and R. R. Gold. "Electromagnetic Wave Propagation Through Magnetoactive Plasmas." Aerospace Corporation, Report No. TDR-69(2119)TR-3, 1962.

3.   R. H. Brown and A. C. B. Lovell. The Exploration of Space by Radio. New York: John Wiley and Sons, Inc., 1958, p. 144.

Aerospace Corporation, El Segundo, California.
REFLECTION AND TRANSMISSION OF ELECTRO-
MAGNETIC WAVES FROM INHOMOGENEOUS
MAGNETOACTIVE PLASMA SLABS, prepared by
Richard R. Gold. 29 March 1963. [71]p. incl. illus.
(Report TDR-169(3230-11)TN-12;SSD-TDR-63-54)
(Contract AF 04(695)-169)   Unclassified report

Exact solutions for the reflection and transmission
coefficients are obtained for two general electron
density distributions: kinked-trapezoid (Fig. 1) and
exponential-homogeneous-exponential (Fig. 5).
Normal incidence into a stratified plasma slab is
assumed so that the electromagnetic waves are
propagating parallel to the free electron density
gradients. A constant magnetic field is applied in
the propagation direction. The solutions derived
on this basis are used to evaluate the effect of the
more realistic inhomogeneous plasma model,
parametrically. Specific consideration is given to
               (over)

Aerospace Corporation, El Segundo, California.
REFLECTION AND TRANSMISSION OF ELECTRO-
MAGNETIC WAVES FROM INHOMOGENEOUS
MAGNETOACTIVE PLASMA SLABS, prepared by
Richard R. Gold. 29 March 1963. [71]p. incl. illus.
(Report TDR-169(3230-11)TN-12;SSD-TDR-63-54)
(Contract AF 04(695)-169)   Unclassified report

Exact solutions for the reflection and transmission
coefficients are obtained for two general electron
density distributions: kinked-trapezoid (Fig. 1) and
exponential-homogeneous-exponential (Fig. 5).
Normal incidence into a stratified plasma slab is
assumed so that the electromagnetic waves are
propagating parallel to the free electron density
gradients. A constant magnetic field is applied in
the propagation direction. The solutions derived
on this basis are used to evaluate the effect of the
more realistic inhomogeneous plasma model,
parametrically. Specific consideration is given to
               (over)

---

the analysis of transmission from a re-entry cone. The asymptotic expansion of the exact solution for the kinked-trapezoid profile provides a simplified expression for calculation purposes when L/λ_0 is larger than one. The analysis of problems in which L/λ_0 is much smaller than one is considered in some detail in the final section.

the analysis of transmission from a re-entry cone. The asymptotic expansion of the exact solution for the kinked-trapezoid profile provides a simplified expression for calculation purposes when L/λ_0 is larger than one. The analysis of problems in which L/λ_0 is much smaller than one is considered in some detail in the final section.

the analysis of transmission from a re-entry cone. The asymptotic expansion of the exact solution for the kinked-trapezoid profile provides a simplified expression for calculation purposes when L/λ_0 is larger than one. The analysis of problems in which L/λ_0 is much smaller than one is considered in some detail in the final section.

the analysis of transmission from a re-entry cone. The asymptotic expansion of the exact solution for the kinked-trapezoid profile provides a simplified expression for calculation purposes when L/λ_0 is larger than one. The analysis of problems in which L/λ_0 is much smaller than one is considered in some detail in the final section.